NASA TECHNICAL NOTE

NASA TN D-4718

NASA TN D-4718

ANALYSIS OF INTEGRATED CHARGED PARTICLE ENERGY SPECTRA FROM GRIDDED ELECTROSTATIC ANALYZERS

by

J. Reece Roth
Lewis Research Center

and

Marion Clark
Cornell University

NATIONAL AERONAUTICS AND SPACE ADMINISTRATION • WASHINGTON, D. C. • AUGUST 1968

ANALYSIS OF INTEGRATED CHARGED PARTICLE ENERGY SPECTRA FROM GRIDDED ELECTROSTATIC ANALYZERS

By J. Reece Roth

Lewis Research Center
Cleveland, Ohio

and

Marion Clark

Cornell University
Ithaca, N.Y.

NATIONAL AERONAUTICS AND SPACE ADMINISTRATION

For sale by the Clearinghouse for Federal Scientific and Technical Information
Springfield, Virginia 22151 – CFSTI price $3.00

ABSTRACT

This report relates the shape of the retarding potential curve produced by gridded electrostatic analyzers to the floating potential, the kinetic temperature, and the half-angle subtended in velocity space by the particles. Special emphasis is placed on the case in which the particles are Maxwellianized, but restricted within an "escape cone" in velocity space of half-angle θ_o. The cases of pulsed and steady-state supply of particles are both considered. A computer program is included which produces an iterated best fit of experimental integrated energy spectra to these analytical expressions, and provides the effective values of the kinetic temperature, floating potential, and escape cone angle. A series of experimental runs is analyzed with the computer program as an illustrative example, and the possible sources of error are discussed.

CONTENTS

ANALYSIS OF INTEGRATED CHARGED PARTICLE ENERGY SPECTRA FROM GRIDDED ELECTROSTATIC ANALYZERS

by J. Reece Roth and Marion Clark

Lewis Research Center

SUMMARY

This report presents a systematic means of evaluating the retarding potential curves obtained from gridded electrostatic analyzers. Special emphasis is placed on the case in which the particles have a Maxwellian velocity distribution along a radius in velocity space, but are confined within an "escape cone" in velocity space of half-angle θ_o. Such velocity distributions may result when particles are lost from "magnetic mirror" confinement geometries and also when an isotropic and Maxwellian group of particles passes through a series of slits or apertures.

Analytical expressions are derived for the expected integrated energy spectra as a function of the half-angle θ_o. The two distinct cases of a pulsed and a steady-state supply of particles are considered. The pulsed case would be appropriate to the analysis of a laser-generated plasma, to certain plasmas generated by rapid magnetic compression, or, under certain conditions, to the experiment discussed herein. The steady-state case is appropriate to some of the experiments performed to illustrate the data analysis technique and to other situations of interest in controlled fusion research.

A computer program is included which obtains an iterated best fit of experimental energy spectra to these analytical expressions. This computer program converges on values of the kinetic temperature, floating potential, and escape cone angle which best fit the experimental data. A series of illustrative experimental runs is reduced with the computer program, and the possible sources of error are discussed. By using the computer program to compare the analytical expressions derived herein with experimental retarding potential curves, significantly more information may reliably be obtained about the velocity distribution than is possible with conventional methods of data reduction, which generally yield only the kinetic temperature of the charged particles.

INTRODUCTION

Retarding field electrostatic analyzers have been widely used to determine the distribution of momentum in a flux of charged particles in the fields of plasma physics (refs. 1 to 5), solid-state physics (refs. 6 and 7), and in other applications. The various types of retarding field energy analyzers have been discussed by Simpson (ref. 8), who points out their individual advantages and difficulties. The specific type of retarding field energy analyzer used in the experimental portion of this investigation is the cylindrically symmetric gridded electrostatic analyzer illustrated in figure 1. In use, a flux of charged particles approaches the analyzer from the right. After passing through a grounded aperture plate, which establishes a zero reference for potential, the particles impinge on grid 3, which may be biased to discriminate between and repel all charges of either positive or negative sign. The particles then approach grid 2, which is biased to repel all particles whose momentum in the direction of the analyzer axis is below the value corresponding to the potential on this grid. The particles with momentum above this value pass through grid 2, and then pass through the negatively biased grid 1, whose function is to prevent secondary electrons from leaving the collector. Varying the bias voltage V on grid 2 from zero to a value much higher than that corresponding to the particle kinetic temperature can make the current to the collector produce a retarding poten-

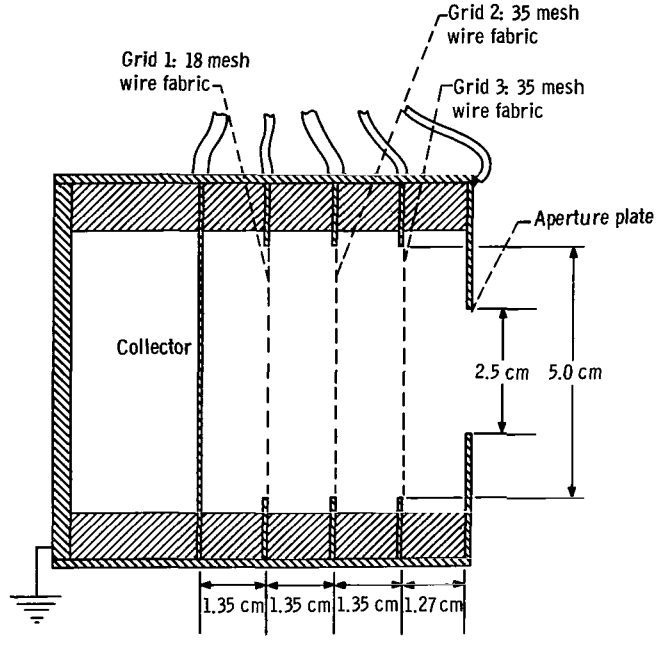

Figure 1. - Schematic drawing of gridded electrostatic analyzer used in experimental investigation.

tial curve of V as a function of collector current. This curve represents the integrated distribution of momentum of particles along the collector axis. Since the analyzer has been assumed to be one dimensional, it will provide information only about the momentum along the analyzer axis, and not necessarily about the total energy of the particles.

In order to establish a one-to-one relation between the particle kinetic temperature and the axial momentum, effects which alter the axial momentum of the particles after they enter the analyzer must be eliminated or accounted for. Much of the existing literature has been devoted to the analysis of such effects. The focusing effect of grids and apertures on the axial momentum of the particles has been considered by Orlinov (ref. 7), Simpson (ref. 8), Simpson and Marton (ref. 9), and Mendlowitz (ref. 10). Space-charge and sheath effects can also alter the axial momentum of the particles if the plasma density between the grids is sufficiently high. Such effects were considered by Mason (ref. 4) and by Fleischmann, et al. (ref. 11). The departure from isotropy of the particle velocity distribution, caused by passage of the particles through successive apertures of the analyzer, was briefly considered by Boyd and Boylett (ref. 5). The effect of a magnetic field on the particle momentum distribution within an analyzer was discussed by Mason (ref. 4), by Simpson (ref. 8), and by Anderson, et al. (ref. 12). The integrated momentum distribution provided by straightforward application of the gridded analyzer is generally deemed not as desirable a form of data presentation as the distribution function of the particles itself. For this reason, means of electronically differentiating the integrated distribution have been developed by Boyd and Boylett (ref. 5), by Leder and Simpson (ref. 6), and by Krawec (ref. 13).

These difficulties and the methods presented for dealing with data affected by them may be said to be well understood when the incident velocity distribution is isotropic in velocity space. There are many applications of the gridded electrostatic analyzer, however, in which the relation between axial momentum and kinetic temperature is complicated by the fact that ions impinging on the analyzer are not isotropically distributed over a hemisphere in velocity space.

This report discusses the results to be expected when the particles reaching the probe are "isotropic" within a cone in velocity space, as shown in figure 2. Such a velocity distribution may arise among the particles that escape through the ends of a "magnetic mirror" containment geometry. Measurements made in such an experimental configuration have been reported by Eubank (ref. 1), Roth (ref. 2), and Zubov, et al. (ref. 14). The analytical form of the integrated momentum distribution does not seem to be available in the literature, except for a special case quoted without derivation by Eubank (ref. 1, p. 100). Analytical expressions are derived in the following analysis which relate the integrated spectrum of axial momentum observed by the collector to the effective escape cone angle, the floating potential, and the kinetic temperature of the particles as they are incident on the analyzer. Because these curves are not simple expo-

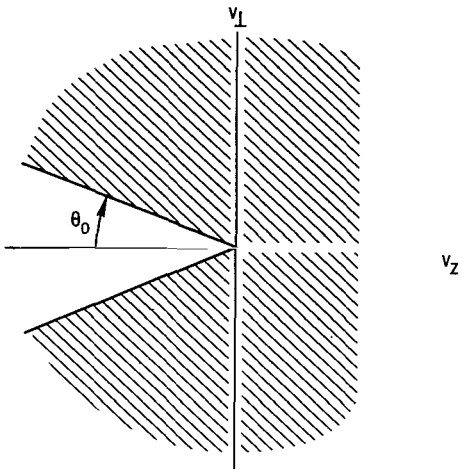

Figure 2. - Schematic drawing of velocity space with particles confined to escape cone of half-angle θ_0.

nentials, a computer program (SPECTR) was written to obtain a best fit of the analytical expressions to the experimentally determined integrated spectrum. This program, written by Loretta R. Ellis, is presented in appendix B.

ANALYTICAL CONSIDERATIONS

Integrated Steady-State Spectra from Arbitrary Cone in Velocity Space

In this section, it is assumed that the particles at the analyzer obey the Maxwellian distribution of velocities along a radius in velocity space and are "isotropic" within a cone in velocity space of half-angle θ_0. It is also assumed that the velocity distribution is axisymmetric about φ, the azimuthal angle in velocity space. This is equivalent to the assumption that the particle motion in the magnetic field is "adiabatic" in the sense of preserving the magnetic moment of the particle (refs. 15 and 16), so that at a particular location of the analyzer with respect to the plasma, the "escape cone" angle θ_0 is not a function of particle energy. In order to make possible an analytical study of the integrated momentum distribution, it is assumed that the magnetic field lines, electric field, and analyzer axis are parallel. The source of this plasma is assumed to float at some potential V_1 with respect to the grounded zero reference of potential at which the analyzer is operated, so that an electric field (parallel to the analyzer axis and the magnetic field) may exist between the plasma source and the analyzer. This floating potential is not that encountered in Langmuir probe theory.

A particular physical situation represented by these assumptions (which represents

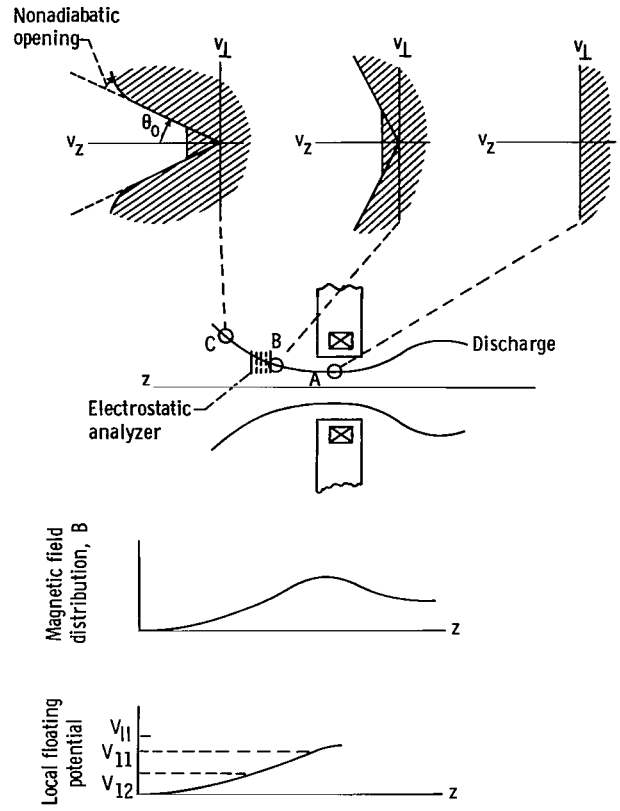

Figure 3. - Schematic drawing showing variation of escape cone angle of particles escaping a magnetic mirror confinement geometry.

the experimental configuration actually used in testing the computer program) is shown in figure 3. The particles move along the magnetic field line and fall through a potential V_{11} (the case of their acquiring energy is illustrated), so that all particles have velocities along the z-axis greater than some minimum value. Because the particles behaved adiabatically in moving to the weaker magnetic field at position B, the escape cone angle is smaller than $\pi/2$. As the particles move to position C, the potential $V_{12} > V_{11}$ through which they fall is greater, and the minimum z-momentum increases further. The escape cone angle becomes still smaller in the much weaker magnetic field at C. It may be so weak that nonadiabatic effects occur (refs. 15 and 16), and the escape cone opens out above its adiabatic value at high particle energies.

The plasma at the analyzer, according to the stated assumptions, will have a distribution function in velocity space given by (ref. 17)

$$dn(v, \theta, \varphi) = \frac{n_o}{\pi^{3/2}} \frac{v^2}{v_o^3} \exp\left(-\frac{v^2}{v_o^2}\right) \sin\theta \, dv \, d\theta \, d\varphi \qquad 0 \le \theta \le \theta_o \tag{1}$$

where the symbols are defined in appendix A. The spatial number density at the analyzer will be n_o only if the distribution is completely isotropic ($\theta_o = \pi$), otherwise the density will be $n_o(1 - \cos \theta_o)/2$. The most probable speed v_o is given in terms of the kinetic temperature $kT = eV_o$ by

$$v_o = \sqrt{\frac{2kT}{m}} = \sqrt{\frac{2eV_o}{m}} \tag{2}$$

With the aid of figure 4, the speed v may be written in terms of the velocity v_z along the analyzer axis,

$$v_z = v \cos \theta \tag{3a}$$

$$v = v_z \sec \theta \tag{3b}$$

If equation (3b) is used to change the variable of integration from v to v_z in equation (1), and an integration over the azimuthal angle $0 \leq \varphi \leq 2\pi$ is performed, one obtains

$$dn(v_z, \theta) = \frac{2n_o}{\pi^{1/2}} \frac{v_z^2}{v_o^3} \exp\left(-\frac{v_z^2 \sec^2\theta}{v_o^2}\right) \sec^3\theta \sin \theta \, dv_z \, d\theta \tag{4}$$

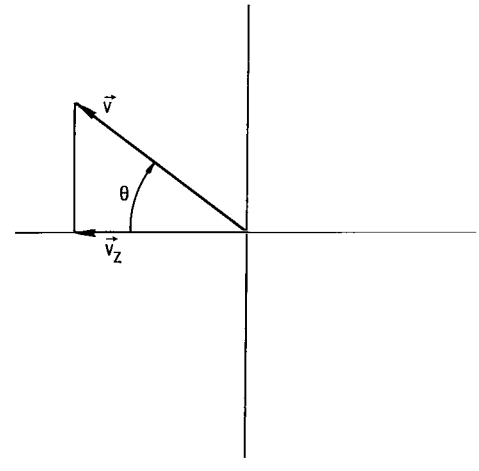

Figure 4. - Geometric relation of velocities.

The differential current density in amperes per square meter of particles impinging on the analyzer is (ref. 17, pp. 206-209)

$$dj(v_z, \theta) = ev \cos \theta \, dn(v, \theta) = ev_z \, dn(v_z, \theta) \tag{5}$$

Substituting equation (4) into equation (5) results in

$$dj(v_z, \theta) = \frac{2n_o e}{\pi^{1/2}} \frac{v_z^3}{v_o^3} \exp\left(-\frac{v_z^2 \sec^2\theta}{v_o^2}\right) \sec^2\theta \tan\theta \, dv_z \, d\theta \tag{6}$$

Integrating this velocity distribution over the cone in velocity space which contains the particles $0 \leq \theta \leq \theta_o$ yields

$$dj(v_z) = \frac{2n_o e}{v_o^3 \pi^{1/2}} \int_0^{\theta_o} v_z^3 \exp\left(-\frac{v_z^2 \sec^2\theta}{v_o^2}\right) \sec^2\theta \tan\theta \, d\theta \, dv_z$$

$$= e \frac{n_o v_z}{\pi^{1/2} v_o} \left[\exp\left(-\frac{v_z^2}{v_o^2}\right) - \exp\left(-\frac{v_z^2 \sec^2\theta_o}{v_o^2}\right)\right] dv_z \tag{7}$$

The current flowing to the collector plate may be determined by integrating equation (7) over all v_z large enough to overcome the potential to which grid 2 is biased. Since the particles may fall through the plasma floating potential V_1, the minimum velocity v_{zmin} is

$$v_{zmin} = \pm\sqrt{\frac{2|eV_1|}{m}} \tag{8}$$

where the plus sign is used if V_1 is positive, and the negative if V_1 is negative. In practice, particles with negative v_z will never reach the analyzer, and the lower limit of integration is zero in this case. The analysis of data can be greatly simplified if $V_1 = 0$. This can be accomplished in an experimental situation by biasing the analyzer ground to equal the floating potential V_1 of the plasma source.

The presence of a floating potential V_1 on the plasma source will result in translat-

ing the abscissa of the integrated energy distribution curve by an amount equal to V_1. When the analyzer is set at some potential $V \geq V_1$, the total transmitted current of positive ions to the collecting electrode is given by integrating equation (7) over the range $v_{zo} \leq v_z \leq \infty$, where

$$v_{zo} \equiv \sqrt{\frac{2e}{m}(V - V_1)} \tag{9}$$

and therefore the total ion current density in amperes per square meter is

$$j = \frac{en_o}{2\pi^{1/2}v_o} \int_{v_{zo}}^{\infty} 2v_z \left[\exp\left(-\frac{v_z^2}{v_o^2}\right) - \exp\left(-\frac{v_z^2 \sec^2\theta_o}{v_o^2}\right) \right] dv_z \tag{10}$$

Performing the integration and substituting equations (2) and (9), one obtains, for the collector current as a function of retarding potential,

$$j = \frac{n_o e v_o}{2\pi^{1/2}} \left\{ \exp\left[-\frac{(V - V_1)}{V_o}\right] - \cos^2\theta_o \exp\left[-\frac{(V - V_1)\sec^2\theta_o}{V_o}\right] \right\} \qquad V \geq V_1 \tag{11}$$

in amperes per square meter. The maximum possible current available to the analyzer occurs when $V = V_1$, because all particles emitted by the source are collected. This current is then given by

$$j_1 = \frac{n_o e v_o}{2\pi^{1/2}} \sin^2\theta_o \tag{12}$$

If equation (12) is written in terms of the average speed $\bar{v}$ of the particles and if the particles are assumed to be isotropically distributed over a hemisphere in velocity space, the result is

$$j_1 = \frac{n_o e \bar{v}}{4} \qquad \theta_o = \frac{\pi}{2} \tag{13}$$

This result for wall bombardment is familiar from kinetic theory (ref. 17, p. 208).

If equation (12) is used to normalize equation (11), one obtains

$$j = j_1 \qquad V \leq V_1 \tag{14}$$

$$\frac{j}{j_1} = \exp\left[-\frac{(V - V_1)}{V_o}\right]\left\{\frac{1 - \cos^2\theta_o \exp\left[-\frac{(V - V_1)\tan^2\theta_o}{V_o}\right]}{\sin^2\theta_o}\right\} \qquad V \geq V_1 \tag{15}$$

Equation (15) is the desired expression for the retarding potential curve. It is a function of the plasma floating potential V_1, the kinetic temperature of the plasma V_o, and the effective escape cone angle in velocity space θ_o. When $V_1 < 0$, the grounded aperture and grid 3 will admit only the "tail" of the velocity distribution, since the low v_z particles will not have sufficient energy to overcome the potential barrier V_1 and reach the analyzer.

Consider some limiting cases of equation (15). When $V_1 \ll V_o$, or if the analyzer ground is biased to the plasma potential so that $V_1 = 0$, equation (15) becomes

$$\frac{j}{j_1} = \frac{\exp\left(-\frac{V}{V_o}\right)}{\sin^2\theta_o}\left[1 - \cos^2\theta_o \exp\left(-\frac{V\tan^2\theta_o}{V_o}\right)\right]_{V_1=0} \qquad V \geq 0 \tag{16}$$

If, in addition, the cone angle θ_o is assumed to be determined by adiabatic motion of the particles from a magnetic mirror maximum B_{max} to the magnetic field existing at the collector B_o, the escape cone angle may be written as (ref. 18)

$$\sin^2\theta_o = \frac{B_o}{B_{max}} \tag{17}$$

From equation (17) it follows that

$$\cos^2\theta_o = \frac{B_{max} - B_o}{B_{max}} \tag{18}$$

and

$$\tan^2\theta_o = \frac{B_o}{B_{max} - B_o} \tag{19}$$

Substituting equations (18) and (19) into equation (16) results in the following equation for the normalized retarding potential curve:

$$\frac{j}{j_1} = \frac{B_{max}}{B_o} \exp\left(-\frac{V}{V_o}\right)\left[1 - \frac{B_{max} - B_o}{B_{max}} \exp\left(-\frac{V}{V_o}\frac{B_o}{B_{max} - B_o}\right)\right] \qquad V_1 = 0 \tag{20}$$

Equation (20) is identical with an expression for the collector current quoted without derivation by Eubank (ref. 1). From the preceding derivation, it is clear that equation (20) holds for the particular case in which the analyzer ground is biased to the floating potential of the plasma, in which the particles move adiabatically along the magnetic field lines, and in which the particle distribution is uniform in angle and Maxwellian in velocity within the escape cone angle θ_o at the location of the probe.

In the limit in which the particles are isotropically distributed over a hemisphere in velocity space, $\theta_o = \pi/2$, and equation (15) becomes simply

$$\frac{j}{j_1} = \exp\left(-\frac{V - V_1}{V_o}\right) \qquad \theta_o = \frac{\pi}{2},\ V \geq V_1 \tag{21}$$

As the escape cone angle becomes very small (as would happen if particles behaved adiabatically in moving from a very strong magnetic field to a very weak field at the analyzer), equation (15) becomes by L'Hôpital's rule (ref. 19, p. 591)

$$\frac{j}{j_1} = \left(\frac{V_o + V - V_1}{V_o}\right)\exp\left(-\frac{V - V_1}{V_o}\right) \qquad \theta_o \to 0,\ V \geq V_1 \tag{22}$$

A comparison of equations (21) and (22) reveals that narrowing the escape cone angle enhances the relative fraction of the particles above any given energy.

Integrated Pulsed Spectra from Arbitrary Cone in Velocity Space

The preceding derivation could be described as assuming a steady state at the analyzer in which the distribution function of the particles is zero outside a cone in velocity space and a Maxwellian function of velocity within it. In the subsequent analysis, a second model is examined in which the arrival rates, averaged over time, are proportional to the number of particles within each velocity increment dv. This situation could come about from the operation of a pulsed plasma source, such as laser-generated plasmas, theta pinches, and the experiment which is described in conjunction with this report. The limits of the cone in velocity space are determined by the geometry of the magnetic field in such applications. The assumption of a Maxwellian distribution, "isotropic" within the velocity space cone, at the site of the analyzer, may not be rigorously true in all experimental situations. However, this assumption is retained along with the other assumptions of the preceding case in order to simplify the analysis. The velocity-space distribution function of particles at the analyzer is obtained from equation (1) and (3b)

$$dn(v_z, \theta, \varphi) = \frac{N_o}{\pi^{3/2}} \frac{v_z^2}{v_o^3} \exp\left(-\frac{v_z^2 \sec^2\theta}{v_o^2}\right) \sec^3\theta \sin\theta \, dv_z \, d\theta \, d\varphi \qquad 0 \le \theta \le \theta_o \tag{23}$$

where the total number of particles reaching the analyzer per pulse is $[N_o(1 - \cos\theta_o)]/2$. One cannot relate N_o directly to a spatial number density at the analyzer because the particles with different velocities will be spread in space. If there are W bursts of particles per second, the collected current in amperes will be

$$di(v_z, \theta) = \frac{2eN_oW}{\pi^{1/2}} \frac{v_z^2}{v_o^3} \exp\left(-\frac{v_z^2 \sec^2\theta_o}{v_o^2}\right) \sec^2\theta \tan\theta \, dv_z \, d\theta \qquad 0 \le \theta \le \theta_o \tag{24}$$

where the integration over the axis of symmetry φ has been performed.

The current collected when the analyzer is set to repel all particles within the escape cone θ_o and with a z-momentum less than that corresponding to v_{zo} is given by

$$i = \frac{2eN_oW}{v_o^3 \pi^{1/2}} \int_{v_{zo}}^{\infty} \int_0^{\theta_o} v_z^2 \exp\left(-\frac{v_z^2 \sec^2\theta}{v_o^2}\right) \sec^2\theta \tan\theta \, dv_z \, d\theta \tag{25}$$

Performing the integration over the angle θ, one obtains

$$i = \frac{eN_o W}{v_o \pi^{1/2}} \int_{v_{zo}}^{\infty} \left[\exp\left(-\frac{v_z^2}{v_o^2}\right) - \exp\left(-\frac{v_z^2 \sec^2\theta_o}{v_o^2}\right) \right] dv_z \tag{26}$$

Performing the integration over v_z and making use of equations (2) and (9) result in

$$i = \frac{eN_o W}{2} \left\{ \operatorname{erfc}\left(\frac{V - V_1}{V_o}\right)^{1/2} - \cos\theta_o \operatorname{erfc}\left[\frac{(V - V_1)\sec^2\theta_o}{V_o}\right]^{1/2} \right\} \qquad V \geq V_1 \tag{27}$$

The maximum possible current to the analyzer occurs when $V = V_1$ and is given by

$$i_1 = \frac{eN_o W}{2} (1 - \cos\theta_o) \tag{28}$$

Using equation (28) to normalize equation (27) gives the shape of the retarding potential curve:

$$i = i_1 \qquad V < V_1 \tag{29}$$

and

$$\frac{i}{i_1} = 1 - \frac{\operatorname{erf}\left(\frac{V - V_1}{V_o}\right)^{1/2} - \cos\theta_o \operatorname{erf}\left[\frac{(V - V_1)}{V_o}\sec^2\theta_o\right]^{1/2}}{1 - \cos\theta_o} \qquad V \geq V_1 \tag{30}$$

The identity $\operatorname{erfc} x \equiv 1 - \operatorname{erf} x$ has been used in equation (30).

Some limiting cases of equation (30) will be examined. When the velocity distribution is isotropic over a hemisphere in velocity space, and $\theta_o = \pi/2$, equation (30) becomes

$$\frac{i}{i_1} = 1 - \operatorname{erf}\left(\frac{V - V_1}{V_o}\right)^{1/2} \qquad V \geq V_1,\ \theta_o = \frac{\pi}{2} \tag{31}$$

On the contrary, when the particles are confined within a very narrow cone in velocity space, equation (30) becomes, by L'Hôpital's rule,

$$\frac{i}{i_1} = \frac{4}{\pi^{1/2}} \int_{x_o}^{\infty} x^2 e^{-x^2}\, dx \qquad V \geq V_1,\ \theta_o \to 0 \tag{32}$$

where

$$x_o = \sqrt{\frac{V - V_1}{V_o}} \tag{33}$$

Other Integrated Energy Spectra

In a particular physical situation, arguments may be available which would lead to prediction of particular types of anisotropic and non-Maxwellian distributions. Calculations similar to those presented for the two preceding models should then be performed. The pertinent details of the plasma processes usually are not well enough understood to justify the choice of an elaborate model. The Maxwellianized plasmas discussed previously may be considered the limiting case of a perfectly random distribution. It is recognized that, in the first case, the assumption of a Maxwellian distribution at the analyzer implies a slightly non-Maxwellian distribution at other axial locations, if adiabatic motion is assumed. The two cases considered are in a way extremes - they give the maximum and minimum arrival rates (and hence V_o) consistent with locally Maxwellian distributions.

It is often of interest to compare these two cases with the opposite limit of a perfectly ordered distribution. Two such ordered distributions were included in the computer program. The first is the delta-function energy distribution shown in figure 5(a). The integrated energy distribution shown in figure 5(b) would be a square wave of the form

$$i = i_1 \qquad V < V_o \tag{34}$$

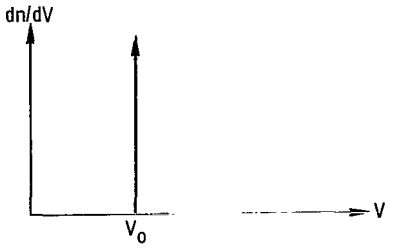

(a) Delta-function energy distribution.

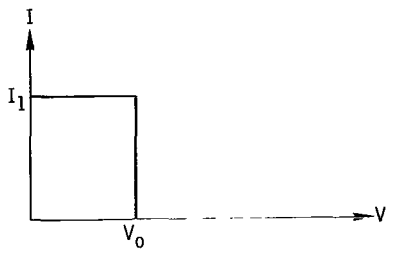

(b) Integrated delta-function distribution.

Figure 5. - Schematic drawing of delta-function energy spectra.

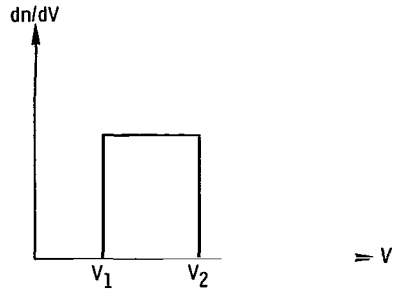

(a) Square-wave distribution function.

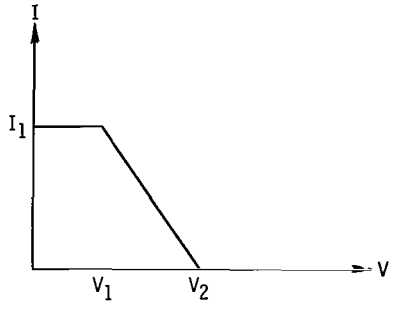

(b) Integrated square-wave distribution.

Figure 6. - Schematic drawing of square-wave energy spectra.

and

$$i = 0 \qquad V \geq V_o \tag{35}$$

This distribution would be appropriate to a perfectly monoenergetic beam of energy V_o (in electron volts), whose velocity is directed along the analyzer axis.

A second simple distribution function is the "square wave" distribution, in which all the particles reaching the analyzer are evenly distributed in energy between $V_1 \leq V \leq V_2$, as illustrated in figure 6(a). The particles have only a negligible spread in angle in velocity space about the analyzer axis. Such a particle distribution will yield the integrated distribution shown in figure 6(b), whose analytic form is

$$i = i_1 \qquad V < V_1 \tag{36}$$

$$i = i_1\left(\frac{V_2 - V}{V_2 - V_1}\right) \qquad V_1 \leq V \leq V_2 \tag{37}$$

$$i = 0 \qquad V > V_2 \tag{38}$$

An average "temperature" for this distribution can be defined by

$$V_o = \frac{1}{2}(V_2 - V_1) \tag{39}$$

COMPUTER PROGRAM FOR DATA ANALYSIS

Equations (15) and (30) for the integrated energy spectra are smooth, monotonically decreasing functions of the retarding potential V. Unfortunately, experimental data obeying these analytical relations cannot be reduced in any simple way, since the curves are not, in general, simple exponentials. In the special case of an isotropic steady-state distribution over the entire hemisphere in velocity space, equation (21) shows that the integrated distribution is exponential. The kinetic temperature of the plasma in question may then be determined by plotting the data on a semilogarithmic graph and measuring the slope of the resulting straight line. When $\theta_o \neq \pi/2$, however, the integrated energy spectra can depart significantly from an exponential curve, and an attempt to force an exponential fit may result in erroneous values of the kinetic temperature V_o, and/or the floating potential V_1.

A computer program was written which provides an iterated best fit of the four integrated energy spectra discussed previously to a tabulated set of experimental data. This computer program, its operation, and its application to data analysis are discussed in appendix B. The integrated distribution functions actually written into the computer program are as follows: In the steady-state case, from equation (15),

$$I = I_o + I_1 \qquad V < V_1 \tag{40}$$

$$I = I_o + I_1 \frac{\exp\left(-\dfrac{V - V_1}{V_o}\right)}{\sin^2\theta_o}\left\{1 - \cos^2\theta_o \exp\left[-\frac{(V - V_1)\tan^2\theta_o}{V_o}\right]\right\} \qquad V \geq V_1 \tag{41}$$

For the pulsed case, from equation (30),

$$I = I_o + I_1 \qquad V < V_1 \tag{42}$$

$$I = I_o + I_1\left\{1 - \frac{\operatorname{erf}\left(\frac{V - V_1}{V_o}\right)^{1/2} - \cos\theta_o \operatorname{erf}\left[\frac{(V - V_1)\sec^2\theta_o}{V_o}\right]^{1/2}}{1 - \cos\theta_o}\right\} \qquad V \geq V_1 \qquad (43)$$

For the delta-function distribution, from equations (34) and (35),

$$I = I_o + I_1 \qquad V < V_o \qquad (44)$$

$$I = I_o \qquad V \geq V_o \qquad (45)$$

For the "square-wave" distribution, from equations (36) to (38),

$$I = I_o + I_1 \qquad V < V_1 \qquad (46)$$

$$I = I_o + I_1\left(\frac{V_2 - V}{V_2 - V_1}\right) \qquad V_1 \leq V \leq V_2 \qquad (47)$$

$$I = I_o \qquad V > V_2 \qquad (48)$$

In the preceding equations, the parameter I_o represents the zero-offset of the curve on the y-axis and can be made less than a few percent of I_1 by zeroing the X-Y recorder before each run.

The computer program takes as input the retarding potential curves in the form of a table of values of V and its corresponding collector current I. Through an iterative process, the program converges to best-fitting values of the five parameters I_o, I_1, V_o, V_1, and θ_o, appropriate to the distribution function in question. The computer output illustrated in table I consists of the raw data for V and I in the first two columns, and the best-fitting curve points for the four distributions given in equations (40) to (48) in the next four columns. Each row of the output table represents one value of this retarding potential at which a point was tabulated from the original X-Y recording. At the bottom of each column the best fitting values of I_o, I_1, V_o, V_1, and θ_o for that distribution are printed out. The mean square error of the best-fitting curve is also printed out.

The parameter I_1 represents the total flux of particles reaching the analyzer, when

TABLE I. - EXAMPLE OF OUTPUT FROM COMPUTER PROGRAM

[V is in volts and I is in amperes $\times 10^{-8}$.]

RUN NUMBER AS-3

	V	I	STEADY	SQ-WAVE	DELTA	PULSED
1	0.	0.14100E 03	0.14121E 03	0.12154E 03	0.89541E 02	0.14417E 03
2	50.000	0.13400E 03	0.12784E 03	0.11544E 03	0.89541E 02	0.12897E 03
3	100.000	0.11780E 03	0.11570E 03	0.10934E 03	0.89541E 02	0.11559E 03
4	150.000	0.10200E 03	0.10471E 03	0.10324E 03	0.89541E 02	0.10381E 03
5	200.000	0.92300E 02	0.94746E 02	0.97137E 02	0.89541E 02	0.93402E 02
6	250.000	0.82500E 02	0.85721E 02	0.91037E 02	0.89541E 02	0.84189E 02
7	300.000	0.75000E 02	0.77547E 02	0.84937E 02	0.89541E 02	0.76004E 02
8	350.000	0.69000E 02	0.70142E 02	0.78837E 02	0.89541E 02	0.68710E 02
9	400.000	0.63000E 02	0.63435E 02	0.72737E 02	0.89541E 02	0.62188E 02
10	450.000	0.56600E 02	0.57359E 02	0.66637E 02	0.89541E 02	0.56342E 02
11	500.000	0.51750E 02	0.51856E 02	0.60537E 02	0.99946E 01	0.51088E 02
12	550.000	0.46500E 02	0.46871E 02	0.54437E 02	0.99946E 01	0.46355E 02
13	600.000	0.44250E 02	0.42356E 02	0.48337E 02	0.99946E 01	0.42083E 02
14	650.000	0.37500E 02	0.38265E 02	0.42237E 02	0.99946E 01	0.38220E 02
15	700.000	0.33000E 02	0.34560E 02	0.36137E 02	0.99946E 01	0.34721E 02
16	750.000	0.30000E 02	0.31205E 02	0.30037E 02	0.99946E 01	0.31547E 02
17	800.000	0.27000E 02	0.28165E 02	0.23937E 02	0.99946E 01	0.28664E 02
18	850.000	0.25000E 02	0.25411E 02	0.17837E 02	0.99946E 01	0.26042E 02
19	900.000	0.22500E 02	0.22917E 02	0.11737E 02	0.99946E 01	0.23656E 02
20	950.000	0.21000E 02	0.20658E 02	0.56365E 01	0.99946E 01	0.21480E 02
21	1000.000	0.19000E 02	0.18611E 02	0.46745E 01	0.99946E 01	0.19496E 02
22	1050.000	0.17000E 02	0.16757E 02	0.46745E 01	0.99946E 01	0.17685E 02
23	1100.000	0.16000E 02	0.15078E 02	0.46745E 01	0.99946E 01	0.16030E 02
24	1150.000	0.14500E 02	0.13557E 02	0.46745E 01	0.99946E 01	0.14517E 02
25	1200.000	0.13500E 02	0.12180E 02	0.46745E 01	0.99946E 01	0.13132E 02
26	1250.000	0.12500E 02	0.10932E 02	0.46745E 01	0.99946E 01	0.11865E 02
27	1300.000	0.11000E 02	0.98012E 01	0.46745E 01	0.99946E 01	0.10703E 02
28	1350.000	0.10500E 02	0.87773E 01	0.46745E 01	0.99946E 01	0.96392E 01
29	1400.000	0.10000E 02	0.78498E 01	0.46745E 01	0.99946E 01	0.86632E 01
30	1450.000	0.90000E 01	0.70097E 01	0.46745E 01	0.99946E 01	0.77677E 01
31	1500.000	0.85000E 01	0.62487E 01	0.46745E 01	0.99946E 01	0.69458E 01
32	1550.000	0.75000E 01	0.55593E 01	0.46745E 01	0.99946E 01	0.61911E 01
33	1600.000	0.70000E 01	0.49349E 01	0.46745E 01	0.99946E 01	0.54977E 01
34	1650.000	0.60000E 01	0.43693E 01	0.46745E 01	0.99946E 01	0.48605E 01
35	1700.000	0.55000E 01	0.38570E 01	0.46745E 01	0.99946E 01	0.42747E 01
36	1750.000	0.50000E 01	0.33930E 01	0.46745E 01	0.99946E 01	0.37360E 01
37	1800.000	0.45000E 01	0.29726E 01	0.46745E 01	0.99946E 01	0.32404E 01
38	1850.000	0.40000E 01	0.25918E 01	0.46745E 01	0.99946E 01	0.27843E 01
39	1900.000	0.35000E 01	0.22469E 01	0.46745E 01	0.99946E 01	0.23645E 01
40	1950.000	0.30000E 01	0.19345E 01	0.46745E 01	0.99946E 01	0.19780E 01
41	2000.000	0.30000E 01	0.16515E 01	0.46745E 01	0.99946E 01	0.16219E 01
42	2050.000	0.20000E 01	0.13952E 01	0.46745E 01	0.99946E 01	0.12940E 01
43	2100.000	0.10000E 01	0.11630E 01	0.46745E 01	0.99946E 01	0.99174E 00
44	2150.000	0.10000E 01	0.95268E 00	0.46745E 01	0.99946E 01	0.71319E 00
45	2200.000	0.50000E 00	0.76217E 00	0.46745E 01	0.99946E 01	0.45640E 00
46	2250.000	0.	0.58960E 00	0.46745E 01	0.99946E 01	0.21961E 00
47	2300.000	0.	0.43329E 00	0.46745E 01	0.99946E 01	0.12210E-02
48	2350.000	-0.50000E 00	0.29170E 00	0.46745E 01	0.99946E 01	-0.20023E 00
49	2400.000	-0.10000E 01	0.16344E 00	0.46745E 01	0.99946E 01	-0.38610E 00
50	2450.000	-0.10000E 01	0.47266E-01	0.46745E 01	0.99946E 01	-0.55762E 00
51	2500.000	-0.15000E 01	-0.57967E-01	0.46745E 01	0.99946E 01	-0.71593E 00

	INITIAL	STEADY	SQ-WAVE	DELTA	PULSED
I0 =	-0.80000E 01	-0.10700E 01	0.46745E 01	0.99946E 01	-0.26540E 01
I1 =	0.14500E 03	0.22431E 03	0.12403E 03	0.79546E 02	0.23439E 03
V0 =	0.35000E 03	0.50544E 03	0.50833E 03	0.50000E 03	0.70571E 03
V1 =	0.30000E 02	-0.27732E 03	-0.58784E 02	0.	-0.23686E 03
THETA =	0.40000E 02	0.72591E 02	0.	0.	0.69349E 02
ERROR =		0.12815E 01	0.54365E 01	0.12354E 02	0.10056E 01

the retarding potential is $V = V_1$. In the case of a steady-state flux, I_1 can be written by using equation (12),

$$I_1 = \frac{n_o e v_o A}{2\pi^{1/2}} G \sin^2\theta_o \tag{49}$$

and by using equation (28) for the pulsed case,

$$I_1 = \frac{eN_o W}{2} (1 - \cos\theta_o) \tag{50}$$

The area of the analyzer opening is A, and the factor G in equation (49) accounts for geometrical effects in the analyzer, such as the transmissivity of the grids. The velocity v_o can be calculated from the kinetic temperature V_o of the plasma, and equation (49) then gives I_1 as proportional to the number density n_o of the plasma source. The parameter V_1 is the effective floating potential of the plasma source at the particular field line on which the analyzer is located, and θ_o is the effective escape cone angle of the particles as they enter the analyzer. It should always be kept in mind that the best-fitting values of I_o, I_1, V_o, V_1, and θ_o are effective values only. These values can be identified with the actual properties of the plasma only when the physical model is applicable and when the systematic errors that might affect them are negligible.

The computer program requires starting values for I_o, I_1, V_o, and V_1 (a universal starting value of $\theta_o = 40^o$ is written into the program). It is not necessary to make very precise estimates of these quantities, since the computer program will converge to the best-fitting values even if the initial estimates are off by a factor of 2 or more. It is not difficult with a little practice to examine an X-Y plot of the retarding I against V curve, and estimate I_o and I_1 by inspection to within 5 percent, and V_o and V_1 to within a factor of 2, when V_1 is positive. The computer time required for an iterated fit to a set of experimental data was about 6 seconds on an IBM 7094II/7044 direct couple computer system.

Experience showed that at least 12 points should be read along the I against V retarding potential curves in order for the computer program to obtain a good fit. The tabulated data points which form the input to the program should be taken at evenly spaced intervals of V along the entire retarding potential curve. If the data points were bunched in a particular region of the retarding-potential curve, the computer program would weigh that region proportionately more heavily than regions with only a few data points.

The mean square error is based on the difference of the entire best-fitting curve and the raw data normalized to the value of I when $V = 0$. A mean square error of 1 per-

cent, for example, means that the average data point deviates from the best-fitting curve by an amount that is 1 percent of I when the retarding potential is zero. Plotting a large number of best-fitting curves on the corresponding I - V data plots showed that a mean square error of less than 1 percent was a very good fit, 1 to 1.5 percent was a good fit, 1.5 to 2.0 percent was only a fair fit, and greater than 2 percent was a relatively poor fit. As the mean square error becomes progressively greater than 1.5 percent, it becomes progressively more probable that either the velocity distribution is non-Maxwellian, or that some systematic error has affected the retarding-potential curve.

EXPERIMENTAL APPARATUS AND PROCEDURE

Description of Apparatus

The superconducting magnet facility in which the experimental data were taken has been described previously (ref. 20). The properties of the plasma and the means used to generate it have been described elsewhere (refs. 2 and 21). The discharge characteristics depend on anode voltage, vacuum tank pressure, etc. Of relevance to the present discussion is the observation of strong turbulence in the plasma, which apparently provides the means of randomizing the velocity distribution, increasing the kinetic temperature through turbulent heating, and scattering particles from this randomized distribution into the escape cone (ref. 21).

A scale drawing of the analyzer used in the experiments to be described subsequently is shown in figure 1. The circuitry and location of the analyzer are shown in figure 7.

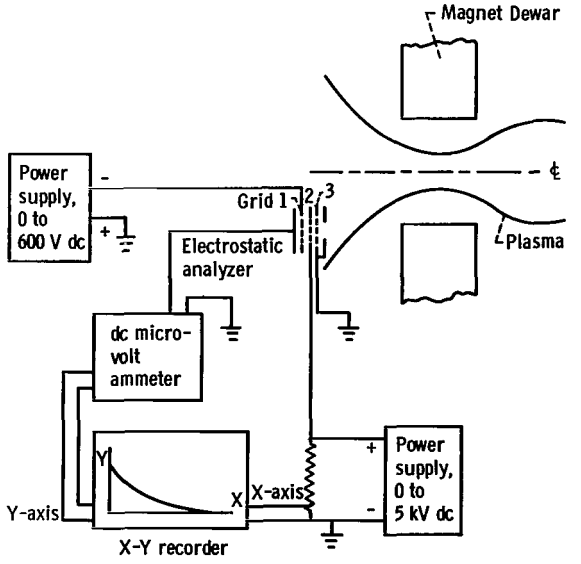

Figure 7. - Schematic drawing of circuitry for electrostatic analyzer.

The analyzer is mounted on a movable support which enables it to be displaced in a direction perpendicular to the axis of the magnetic field in a plane containing the magnetic field axis. An X-Y recorder was used to record the retarding potential curves in the present experiment. A fast-sweep oscilloscope display would be desirable in an experiment of short duration.

Experimental Procedure

The front surface of the analyzer was placed 20 centimeters away from the point of maximum magnetic field. The axis of the probe was parallel to the magnetic field axis but displaced radially 10 centimeters from it. This placement was deemed desirable because the ion current impinging on the analyzer near the magnetic field axis was too noisy to produce smooth retarding potential curves of high quality. Unfortunately this placement resulted in the introduction of a systematic error in the effective escape cone angle θ_o, since the analyzer axis was at an angle of about 30^o to the local magnetic field lines.

The field strength at the magnetic field maximum was 1.0 tesla, about 0.15 tesla at the front surface of the analyzer and about 0.10 tesla at the collector. The magnetic fields at the location of the energy probe were small enough to cause nonadiabatic effects among ions of the kinetic temperatures observed (refs. 15 and 16), and one would therefore not necessarily expect ions of high energy to be confined to an escape cone whose angle is given by equation (17).

The plasma was observed to float at a potential that is typically from $-300 \leq V_1 \leq 200$ volts. The electron energies within the plasma appeared to be about equal to the floating potential.

The collector currents were in all cases below 10^{-5} ampere, and the corresponding number density of particles in the beam was below 10^6 particles per cubic centimeter for the results presented herein. The minimum electron Debye length was larger than the analyzer diameter, and the local value of the ion gyroradius, corresponding to the ion kinetic temperature, was much larger than the diameter of the grid holes.

During operation, the 2.54-centimeter-diameter aperture and grid 3 were grounded, as shown on figure 7. Grid 3 was used in preliminary measurements to verify that the electron current reaching the analyzer was much smaller than the ion current. Grid 2 was connected to a well-filtered 5-kilovolt d-c power supply. This power supply could be varied from zero to full scale by a motor drive and variable transformer in the power supply primary circuit. This assured that the retarding potential appearing on grid 2 would vary smoothly and continuously in time. Grid 1 was biased from -200 to -600 volts dc. Its function was the repelling of secondary electrons that might be emitted by ions that struck the collector, and also the repelling of any electrons below this energy that

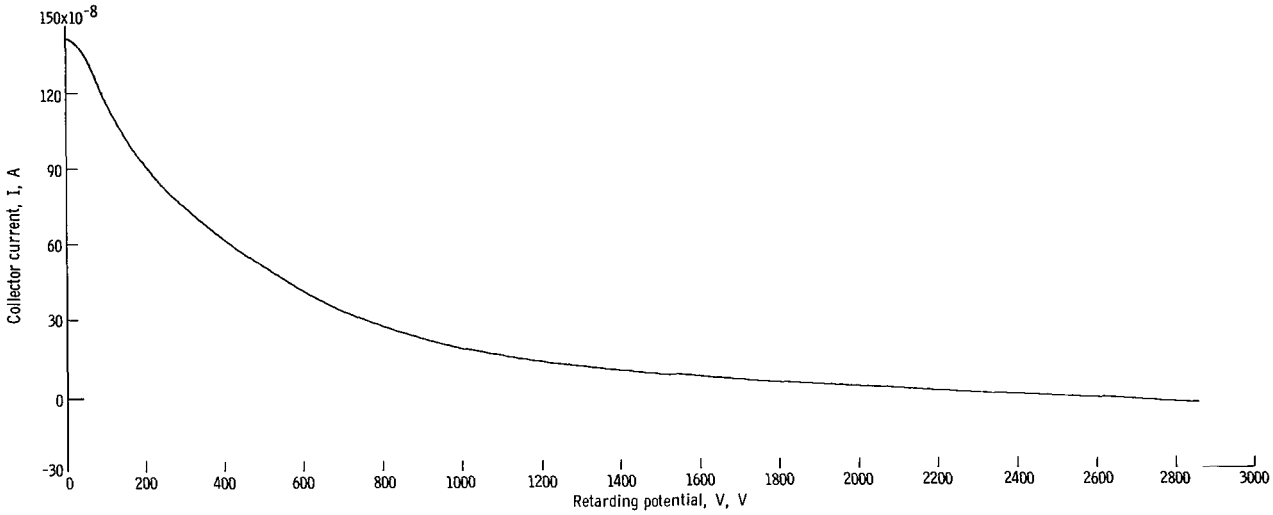

Figure 8. - Typical raw integrated data from run AS-3.

entered with the ion beam. The collector was a flat brass disk that was connected to an electronic microvolt-ammeter. The output of this instrument was fed into the Y-axis of an X-Y recorder. The X-axis of the recorder was driven by a voltage proportional to the retarding potential applied on grid 2. Approximately 1 minute was required to sweep out a complete retarding-potential curve.

The X-Y graphs of the retarding potential curves, illustrated in figure 8, were converted to tabular form by picking and tabulating approximately 50 values of the collector current for evenly spaced values of the retarding potential. An estimate was then made of the values of I_o, I_1, V_o, and V_1 to start the iterative process. These data were then placed on punched cards and used as input to the computer program.

EXPERIMENTAL RESULTS

Illustrative Experimental Data

Four series of experimental runs, whose characteristics are summarized in table II, were taken with the energy analyzer. A run consisted of taking a single retarding potential curve; a series consisted of many runs taken under the same set of operating conditions. These series of runs illustrate the application of the computer program to an actual set of experimental data and make it possible to investigate the magnitude of the systematic and random errors encountered in practice.

The second column of table II lists the number of runs taken in each series. Each series listed in table II was made on the same day, in sequence, and under conditions

TABLE II. - OPERATING PARAMETERS FOR RUN SERIES INVESTIGATED

Run series	Number of runs in series	Gas used	Tank pressure		Bias voltage on grid 1, V	Anode current, A	Elapsed time for series, min	x-axis scale, retarding potential on grid 2, V/in.	y-axis scale, collector current, A/in.
			torr	N/m^2					
AS	10	Helium	9×10^{-6}	1.2×10^{-3}	-200	0.005	76	200	3×10^{-7}
AT	10	Helium	4.9×10^{-5}	6.5×10^{-3}	-500	.061	36	200	10^{-6}
AU	13	Neon	1.9×10^{-6}	2.5×10^{-4}	-500	.010	43	200	10^{-7}
AV	13	Neon	4.0×10^{-6}	5.3×10^{-4}	-500	.030	40	200	3×10^{-7}
CK-CL	26	Deuterium	9.0×10^{-6}	1.2×10^{-3}	-600	.004	--	500	10^{-7}
CM-CN	17	Deuterium	1.2×10^{-5}	1.6×10^{-3}	-600	.0025	--	200	10^{-7}

(vacuum tank pressure, plasma number density, etc.,) that were as nearly identical as the nature and limitations of the apparatus would permit. The duration over which a series was taken is listed in the seventh column of table II. The quantity that was observed to vary most during a series of runs was the vacuum tank pressure. The bias voltage used on grid 1 to repel secondary electrons emitted from the collector is listed in column 5. The scales of the ordinate and abscissa of the retarding potential curves from the X-Y recorder are shown in the last two columns of table II. A typical X-Y plot of the retarding potential from the AS series of runs is shown in figure 8.

Computer Generated Best-Fitting Integrated Spectra

The experimental retarding potential curves described for the first four series of runs listed in table II (altogether 46 curves) were tabulated and used as input to the computer program, which then obtained best-fitting theoretical curves. The computer output for the experimental run AS-3, shown in figure 8, is given in table I. Data were read from the curve in figure 8 for 51 values of the retarding potential V. These raw data points of the retarding potential V and collector current I then appear in the first two columns of table I. From 12 to 20 data points are sufficient to define the shape of the curve for use by the computer program. Between 50 and 60 raw data points were used for each run listed in table II, since these runs were being used for illustrative purposes and also because it was desired to eliminate an inadequate number of points as a possible source of error.

The last four columns in table I are the analytical curves that best fit the experimental data for the four possible integrated energy spectra discussed previously. At the bottom of table I are shown the best-fitting values of I_o, I_1, V_o, V_1, and θ_o for the four

TABLE III. - ANALYSIS OF AS RUN SERIES

(a) Parameters for best-fitting steady curve

AS series run number	y-axis zero offset, I_o, A	Total particle flux reaching analyzer, I_1, A	Kinetic temperature, V_o, eV/ion	Floating potential, V_1, V	Effective escape cone angle in velocity space, θ_o, deg	Mean square error, percent	Elapsed time, min	Tank pressure, torr	Tank pressure, N/m^2
3	-1.07×10^{-8}	224×10^{-8}	505	-277	73	1.28	9	9.1×10^{-6}	1.21×10^{-3}
6	-1.53	218	501	-303	69	1.49	22	↓	↓
9	-.36	268	508	-355	85	1.36	33		
12	-1.60	251	510	-325	83	1.46	43		
15	-1.14	215	513	-335	67	1.36	51	9.0×10^{-6}	1.195×10^{-3}
18	-.48	235	506	-345	73	1.53	59	9.0	1.195
20	-.77	244	526	-362	78	1.37	64	8.85	1.175
22	-.67	286	519	-446	76	1.49	68	8.80	1.17
24	-1.07	229	515	-332	72	1.73	72	9.0	1.195
26	.65	231	493	-326	72	1.29	76	9.05	1.20
Average	-0.80×10^{-8}	240×10^{-8}	510	-341	75	1.44	--	9.01×10^{-6}	1.196×10^{-3}
Mean error	$\pm0.48\times10^{-8}$	$\pm18\times10^{-8}$	±7	±19	±5	±0.10	--	0.08×10^{-6}	0.016×10^{-3}

(b) Parameters for best-fitting pulsed curve

AS series run number	y-axis zero offset, I_o, A	Total particle flux reaching analyzer, I_1, A	Kinetic temperature, V_o, eV/ion	Floating potential, V_1, V	Effective escape cone angle in velocity space, θ_o, deg	Mean square error, percent
3	-2.65×10^{-8}	234×10^{-8}	706	-237	69	1.01
6	-3.04	339	697	-265	85	1.04
9	-2.21	223	736	-198	75	.85
12	-3.09	331	708	-275	84	1.08
15	-2.58	297	709	-291	78	.98
18	-1.79	341	693	-297	84	1.13
20	-2.10	357	718	-314	87	.96
22	-2.03	366	710	-308	88	1.11
24	-2.49	238	714	-266	71	1.41
26	-.80	290	681	-279	77	.92
Average	-2.28×10^{-8}	302×10^{-8}	707	-273	80	1.05
Mean error	$\pm0.49\times10^{-8}$	$\pm42\times10^{-8}$	±10	±25	±6	±0.12

(c) Parameters for best-fitting square-wave curve

AS series run number	y-axis zero offset, I_o, A	Total particle flux reaching analyzer, I_1, A	Kinetic temperature, V_o, eV/ion	Floating potential, V_1, V	Mean square error, percent
3	4.67×10^{-8}	124×10^{-8}	508	-59	5.44
6	3.87	125	534	-111	5.61
9	5.17	122	532	-106	5.53
12	3.98	124	540	-119	5.56
15	4.42	123	549	-134	5.56
18	4.82	122	550	-142	5.58
20	4.66	122	584	-168	5.58
22	4.99	122	554	-144	5.68
24	4.62	123	543	-122	5.83
26	6.43	120	506	-97	5.47
Average	4.76×10^{-8}	123×10^{-8}	540	-120	5.58
Mean error	$\pm0.35\times10^{-8}$	$\pm1.1\times10^{-8}$	±16	±22	±0.07

(d) Parameters for best-fitting delta-function curve

AS series run number	y-axis zero offset, I_o, A	Total particle flux reaching analyzer, I_1, A	Kinetic temperature, V_o, eV/ion	Mean square error, percent
3	10.0×10^{-8}	79.5×10^{-8}	500	12.4
6	8.92	76.0		12.1
9	10.2	74.9		12.2
12	9.41	73.5		12.4
15	9.08	75.2		12.3
18	9.67	72.2		12.1
20	10.0	72.1		12.2
22	9.90	72.1		12.3
24	9.72	74.1		12.6
26	11.9	74.9	450	12.3
Average	9.88×10^{-8}	74.5×10^{-8}	495	12.3
Mean error	$\pm0.43\times10^{-8}$	$\pm1.7\times10^{-8}$	±9	±0.1

TABLE IV. - ANALYSIS OF AT RUN SERIES

(a) Parameters for best-fitting steady curve

AT series run number	y-axis zero offset, I_o, A	Total particle flux reaching analyzer, I_1, A	Kinetic temperature, V_o, eV/ion	Floating potential, V_1, V	Effective escape cone angle in velocity space, θ_o, deg	Mean square error, percent	Elapsed time, min	Tank pressure	
								torr	N/m^2
1	-13.9×10^{-8}	812×10^{-8}	391	-46	44	0.75	0	4.95×10^{-5}	6.60×10^{-3}
3	-12.5	784	367	-43	41	.77	4		
5	-10.4	789	365	-35	42	.78	8		
7	-9.9	782	367	-37	42	.76	12		
9	-10.7	773	358	-55	40	.82	16		
11	-10.2	760	347	-48	38	.87	20	4.90×10^{-5}	6.52×10^{-3}
13	-7.9	754	335	-39	38	.82	24	4.95	6.60
15	-15.0	813	401	-63	45	.82	27	4.90	6.52
17	-14.8	794	392	-60	43	.98	31	4.90	6.52
19	-17.6	820	422	-65	45	.90	34	4.90	6.52
Average	-12.3×10^{-8}	788×10^{-8}	375	-49	42	0.83	--	4.93×10^{-5}	6.56×10^{-3}
Mean error	$\pm2.5\times10^{-8}$	$\pm18\times10^{-8}$	±22	±9	±2	±0.06	--	$\pm0.02\times10^{-5}$	0.026×10^{-3}

(b) Parameters for best-fitting pulsed curve

AT series run number	y-axis zero offset, I_o, A	Total particle flux reaching analyzer, I_1, A	Kinetic temperature, V_o, eV/ion	Floating potential, V_1, V	Effective escape cone angle in velocity space, θ_o, deg	Mean square error, percent
1	-17.8×10^{-8}	792×10^{-8}	464	33	41	0.53
3	-16.2	765	435	36	39	.51
5	-14.4	772	435	40	39	.45
7	-14.0	764	437	40	39	.44
9	-14.0	749	419	29	37	.54
11	-13.4	737	409	35	36	.56
13	-11.3	734	396	39	36	.44
15	-18.2	785	468	25	41	.58
17	-18.2	768	458	29	39	.75
19	-21.0	791	493	27	41	.67
Average	-15.9×10^{-8}	766×10^{-8}	441	33	39	0.55
Mean error	$\pm2.4\times10^{-8}$	$\pm16\times10^{-8}$	±23	±5	±1	±0.08

(c) Parameters for best-fitting square-wave curve

AT series run number	y-axis zero offset, I_o, A	Total particle flux reaching analyzer, I_1, A	Kinetic temperature, V_o, eV/ion	Floating potential, V_1, V	Mean square error, percent
1	18.0×10^{-8}	741×10^{-8}	509	-8.0	4.28
3	17.6	740	502	-31.2	4.28
5	19.0	738	493	-16.7	4.38
7	17.5	740	518	-36.1	4.40
9	16.3	741	513	-62.4	4.36
11	15.8	742	516	-71.7	4.35
13	15.4	742	512	-73.1	4.42
15	18.4	739	519	-25.6	4.42
17	17.3	740	529	-43.2	4.40
19	18.2	740	540	-22.8	4.45
Average	17.4×10^{-8}	740×10^{-8}	515	-39.1	4.37
Mean error	$\pm0.9\times10^{-8}$	$\pm1\times10^{-8}$	±9	±18.8	±0.05

(d) Parameters for best-fitting delta-function curve

AT series run number	y-axis zero offset, I_o, A	Total particle flux reaching analyzer, I_1, A	Kinetic temperature, V_o, eV/ion	Mean square error, percent
1	68.5×10^{-8}	501×10^{-8}	500	14.2
3	61.9	486		14.1
5	63.4	492		14.1
7	65.1	488		14.2
9	58.1	470		14.0
11	56.7	467		14.0
13	61.7	482	450	14.1
15	68.6	492	500	14.3
17	67.2	484	500	14.5
19	67.6	483	550	14.4
Average	63.9×10^{-8}	485×10^{-8}	500	14.2
Mean error	$\pm3.5\times10^{-8}$	$\pm7\times10^{-8}$	±10	±0.1

TABLE V. - ANALYSIS OF AU RUN SERIES

(a) Parameters for best-fitting steady curve

AU series run number	y-axis zero offset, I_o, A	Total particle flux reaching analyzer, I_1, A	Kinetic temperature, V_o, eV/ion	Floating potential, V_1, V	Effective escape cone angle in velocity space, θ_o, deg	Mean square error, percent	Elapsed time, min	Tank pressure	
								torr	N/m^2
1	-1.31×10^{-8}	47.6×10^{-8}	683	-326	43	1.38	0	1.7×10^{-6}	2.26×10^{-6}
3	-1.10	58.7	662	-199	60	2.37	7	2.0	2.66
5	-.47	50.6	592	-154	49	.79	9	1.95	2.60
7	-.80	55.9	624	-204	56	.71	13	2.1	2.80
9	-1.17	51.6	703	-387	50	1.15	17	1.6	2.13
11	-1.58	53.5	727	-354	51	1.52	20	1.8	2.40
13	-.40	44.3	530	-70	38	1.11	23	1.95	2.60
15	-.84	48.1	620	-237	45	.79	27	1.85	2.46
17	-.83	50.1	653	-271	48	.71	29	1.90	2.53
19	-.72	53.7	632	-167	53	.87	35	2.6	3.46
21	-1.20	42.5	667	-331	35	.77	39	1.45	1.93
22	-1.44	43.8	696	-394	37	1.17	41	1.50	2.00
23	-.91	46.0	659	-317	41	.99	43	1.55	2.06
Average	-0.98×10^{-8}	49.7×10^{-8}	650	-262	47	1.10	--	1.84×10^{-6}	2.45×10^{-4}
Mean error	$\pm0.29\times10^{-8}$	$\pm4.0\times10^{-8}$	±39	±84	±6	±0.32	--	$\pm0.22\times10^{-6}$	$\pm0.29\times10^{-4}$

(b) Parameters for best-fitting pulsed curve

AU series run number	y-axis zero offset, I_o, A	Total particle flux reaching analyzer, I_1, A	Kinetic temperature, V_o, eV/ion	Floating potential, V_1, V	Effective escape cone angle in velocity space, θ_o, deg	Mean square error, percent
1	-1.40×10^{-8}	43.7×10^{-8}	760	-118	37	1.43
3	-1.19	55.2	785	-91.5	53	2.37
5	-.69	48.2	694	-27.4	44	.85
7	-.89	52.3	730	-85.9	50	.73
9	-1.30	47.1	792	-196.3	43	1.14
11	-1.76	49.5	835	-180	45	1.53
13	-.87	43.8	655	31.2	37	1.37
15	-1.02	44.8	703	-67.5	39	.83
17	-.96	46.2	736	-95.9	41	.73
19	-.96	51.4	752	-49.6	48	.92
21	-1.70	40.7	783	-147	30	.83
22	-1.82	41.9	813	-206	33	1.20
23	-1.21	43.3	756	-137	36	1.03
Average	-1.21×10^{-8}	46.8×10^{-8}	753	-105	41	1.15
Mean error	$\pm0.29\times10^{-8}$	$\pm3.5\times10^{-8}$	±39	±54	±5	±0.33

TABLE V. - Concluded. ANALYSIS OF AU RUN SERIES

(c) Parameters for best-fitting square-wave curve

AU series run number	y-axis zero offset, I_o, A	Total particle flux reaching analyzer, I_1, A	Kinetic temperature, V_o, eV/ion	Floating potential, V_1, V	Mean square error, percent
1	1.77×10^{-8}	41.6×10^{-8}	873	-275	3.86
3	1.94	43.5	647	8.8	4.93
5	2.16	41.6	655	7.29	4.10
7	2.08	41.7	624	9.3	4.32
9	1.87	41.4	850	-290	4.49
11	1.57	42.1	832	-209	4.12
13	2.06	41.6	708	-45	3.65
15	1.76	41.9	783	-165	3.99
17	1.94	41.6	779	-154	4.14
19	2.30	43.0	654	13.9	4.00
21	1.77	41.4	1016	-464	3.98
22	1.54	41.7	1046	-526	3.99
23	1.93	41.3	888	-307	4.00
Average	1.90×10^{-8}	41.9×10^{-8}	797	-184	4.12
Mean error	$\pm0.17\times10^{-8}$	$\pm0.5\times10^{-8}$	±112	±148	±0.21

(d) Parameters for best-fitting delta-function curve

AU series run number	y-axis zero offset, I_o, A	Total particle flux reaching analyzer, I_1, A	Kinetic temperature, V_o, eV/ion	Mean square error, percent
1	4.32×10^{-8}	22.9×10^{-8}	800	13.1
3	4.73	28.9	700	13.8
5	5.23	28.4	650	13.1
7	4.92	28.0	650	12.9
9	4.47	22.4	750	13.3
11	4.17	23.9	800	12.9
13	4.61	26.7	750	12.8
15	4.39	24.6	750	13.3
17	4.59	24.6	750	13.2
19	5.16	28.8	700	12.8
21	4.59	20.9	800	13.7
22	4.30	20.5	800	13.6
23	4.41	22.2	800	13.2
Average	4.61×10^{-8}	24.8×10^{-8}	746	13.2
Mean error	$\pm0.25\times10^{-8}$	$\pm2.6\times10^{-8}$	±44	±0.3

integrated energy distributions considered. As may be seen, the pulsed curve of equation (43) gave a best fit (lowest mean square error) to the experimental data.

The characteristics of the best-fitting curves of each type (steady, pulsed, square wave, and delta function) for each of the four series of runs are listed in tables III to VI. In these tables the best-fitting values of I_o, I_1, V_o, V_1, and θ_o are listed for each individual run. The mean square error for a given run is listed, as are the elapsed time and the vacuum tank pressure appropriate to each run. By examining the run-to-run variations of the parameters in tables III to VI, one may obtain a qualitative feeling for the precision with which V_o, θ_o, etc., can be evaluated by the curve-fitting method used in this report. The greatest run-to-run variation occurs in the parameter I_o. This parameter, however, is not a significant experimental variable, since it merely measures the precision with which one can zero the dc microvolt-ammeter and/or the X-Y recorder. The zero offset represented by I_o was generally about 1 percent of the collector current I_1.

The AS and AT series of runs listed in tables III and IV both were run with helium gas, both had a very small variation of background pressure during the run series, and both gave a best fit for the pulsed production of particles. The AS series is notable in having a very small run-to-run variation of the best-fitting parameters, while the AT series has the lowest observed mean square error (and hence the best fit), for each individual run.

TABLE VI - ANALYSIS OF AV RUN SERIES

(a) Parameters for best-fitting steady curve

AV series run number	y-axis zero offset, I_o, A	Total particle flux reaching analyzer, I_1, A	Kinetic temperature, V_o, eV/ion	Floating potential, V_1, V	Effective escape cone angle in velocity space, θ_o, deg	Mean square error, percent	Elapsed time, min	Tank pressure	
								torr	N/m^2
1	6.53×10^{-8}	181×10^{-8}	196	126	29	1.68	0	4.6×10^{-6}	6.12×10^{-4}
3	7.57	181	193	130	30	1.77	3	4.6	6.12
5	6.59	181	196	129	29	1.78	7	4.75	6.22
7	6.62	185	200	136	31	1.74	10	4.90	6.52
9	5.91	185	206	136	31	1.79	14	4.95	6.58
11	5.84	174	181	136	25	1.79	17	3.9	5.20
13	5.98	174	180	145	25	1.74	21	4.0	5.32
15	6.77	190	208	152	33	1.77	25	5.1	6.80
17	6.36	180	198	140	29	1.66	28	4.8	6.40
19	5.23	178	181	142	28	1.60	31	3.8	5.05
21	5.09	167	170	135	20	1.63	34	3.6	4.80
23	5.84	169	171	132	22	1.74	37	3.7	4.92
25	6.99	176	186	135	26	1.57	41	4.6	6.12
Average	6.26×10^{-8}	179×10^{-8}	190	136	28	1.71	--	4.41×10^{-6}	5.85×10^{-4}
Mean error	$\pm0.52\times10^{-8}$	$\pm5\times10^{-8}$	±11	±5	±3	±0.07	--	$\pm0.47\times10^{-6}$	$\pm0.625\times10^{-4}$

(b) Parameters for best-fitting pulsed curve

AV series run number	y-axis zero offset, I_o, A	Total particle flux reaching analyzer, I_1, A	Kinetic temperature, V_o, eV/ion	Floating potential, V_1, V	Effective escape cone angle in velocity space, θ_o, deg	Mean square error, percent
1	6.16×10^{-8}	180×10^{-8}	235	169	29	1.81
3	7.24	180	231	173	29	1.89
5	6.26	180	235	173	29	1.90
7	6.22	184	241	177	31	1.89
9	5.50	184	249	179	31	1.91
11	5.48	173	218	175	24	1.96
13	5.60	173	218	182	25	1.88
15	6.32	189	251	193	32	1.98
17	5.94	180	239	181	28	1.82
19	4.85	178	219	179	27	1.78
21	4.80	166	203	174	20	1.76
23	5.56	168	204	173	21	1.88
25	6.63	175	224	176	26	1.74
Average	5.89×10^{-8}	178×10^{-8}	228	177	27	1.86
Mean error	$\pm0.55\times10^{-8}$	$\pm5\times10^{-8}$	±13	±4	±3	±0.06

TABLE VI. - Concluded. ANALYSIS OF AV RUN SERIES

(c) Parameters for best-fitting square-wave curve

AV series run number	y-axis zero offset, I_o, A	Total particle flux reaching analyzer, I_1, A	Kinetic temperature, V_o, eV/ion	Floating potential, V_1, V	Mean square error, percent
1	8.89×10^{-8}	185×10^{-8}	335	90	3.09
3	9.89	186	335	88	3.11
5	9.05	185	337	90	3.10
7	9.22	189	336	95	3.04
9	8.83	185	326	120	3.20
11	7.85	197	387	-81	3.30
13	7.97	179	332	94	3.07
15	9.79	192	328	126	2.94
17	8.94	185	338	99	3.01
19	7.55	180	302	122	2.84
21	7.09	201	395	-52	3.27
23	7.87	200	388	-39	3.24
25	9.13	180	333	92	2.92
Average	8.62×10^{-8}	188×10^{-8}	344	65	3.09
Mean error	$\pm0.73\times10^{-8}$	$\pm6\times10^{-8}$	±21	±57	±0.11

(d) Parameters for best-fitting delta-function curve

AV series run number	y-axis zero offset, I_o, A	Total particle flux reaching analyzer, I_1, A	Kinetic temperature, V_o, eV/ion	Mean square error, percent
1	14.9×10^{-8}	146×10^{-8}	400	11.1
3	15.8	147	400	11.1
5	13.6	141	450	10.2
7	14.0	145	↓	10.4
9	13.9	146	↓	10.6
11	11.9	136	↓	10.1
13	13.7	143	400	11.1
15	15.4	152	450	10.8
17	13.9	143	450	10.5
19	12.9	146	400	10.9
21	11.8	135	400	10.6
23	12.6	137	400	10.5
25	13.5	138	450	10.1
Average	13.7×10^{-8}	143×10^{-8}	427	10.6
Mean error	$\pm0.9\times10^{-8}$	$\pm4\times10^{-8}$	±25	±0.3

Run series AU and AV are listed in tables V and VI, respectively. These series are both notable in having a rather large mean square error and a rather large run-to-run variation. It is shown later that this imprecision is probably attributable to the rather large uncontrollable variation in background pressure that occurred during these two series of runs. Such variations in vacuum tank pressure occurred whenever neon gas was used, as it was during these runs.

In figure 9 are shown four runs from the AS series, each of which has the raw data and one of the four types of curve fits drawn on it. An examination of these four typical runs reveals that the best-fitting curves are not necessarily good fits, and that the square-wave and delta-function curves were very poor fits. In no case during this set of 46 runs was either the delta-function or the square-wave distribution the best-fitting curve. It is permissible to conclude from this that the particles from this discharge are much closer to a Maxwellian distribution than they are to a delta-function or square-wave energy distribution function.

In figure 10 are shown one typical run from each of the four series, with the type of curve fit that gave the lowest mean square error for that series. As may be seen, the curve fits were quite good in all cases. Only figure 10(d), which had a mean square error of 1.68 percent, had a really noticeable systematic departure from the raw data. This departure is characteristic of the runs in this series.

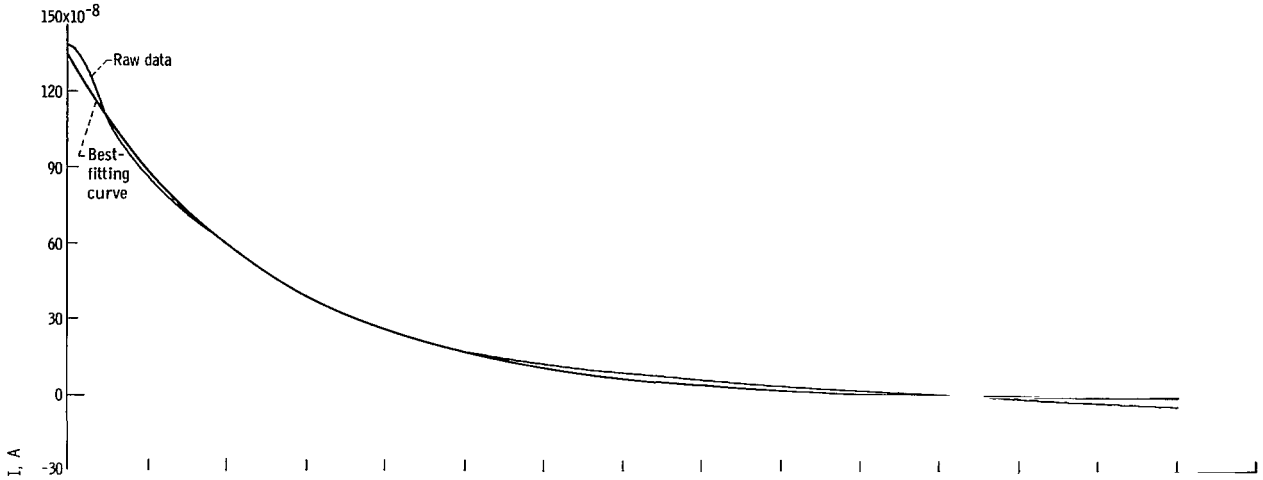

(a) Steady curve. Run AS-6; y-axis zero offset, I_0, -1.53×10^{-8} amperes; total particle flux reaching analyzer, I_1, 218×10^{-8} amperes; kinetic temperature, V_0, 501 electron volts per ion; floating potential, V_1, -303 volts; effective escape cone angle in velocity space, θ_0, 69°; mean square error, 1.49 percent.

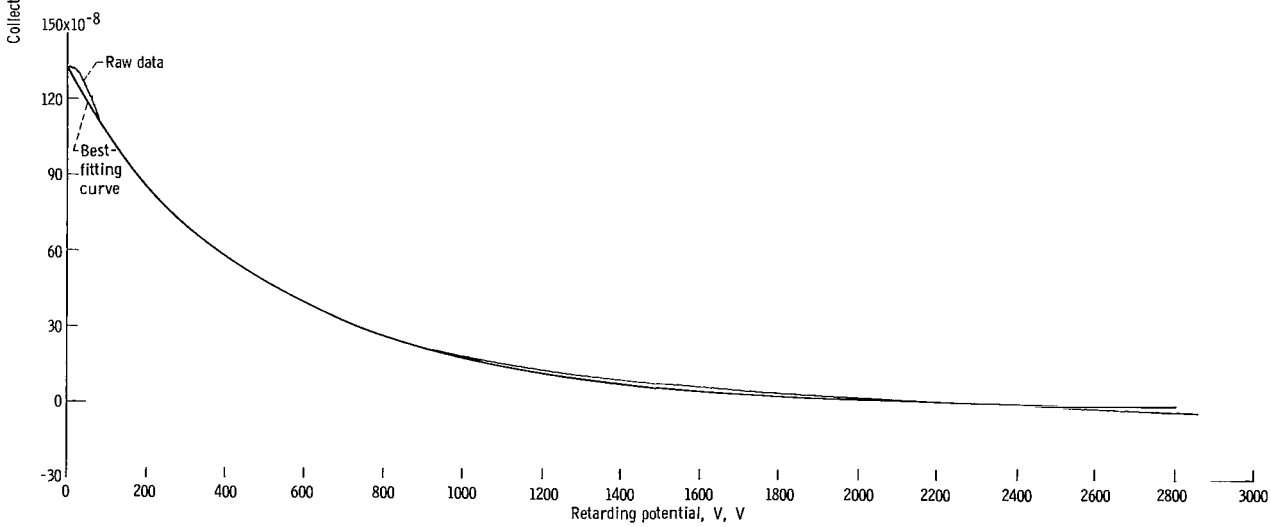

(b) Pulsed curve. Run AS-15; y-axis zero offset, I_0, -2.58×10^{-8} amperes; total particle flux reaching analyzer, I_1, 297×10^{-8} amperes; kinetic temperature, V_0, 709 electron volts per ion; floating potential, V_1, -291 volts; effective escape cone angle in velocity space, θ_0, 78°; mean square error, 0.98 percent.

Figure 9. - Best-fitting curves of each type.

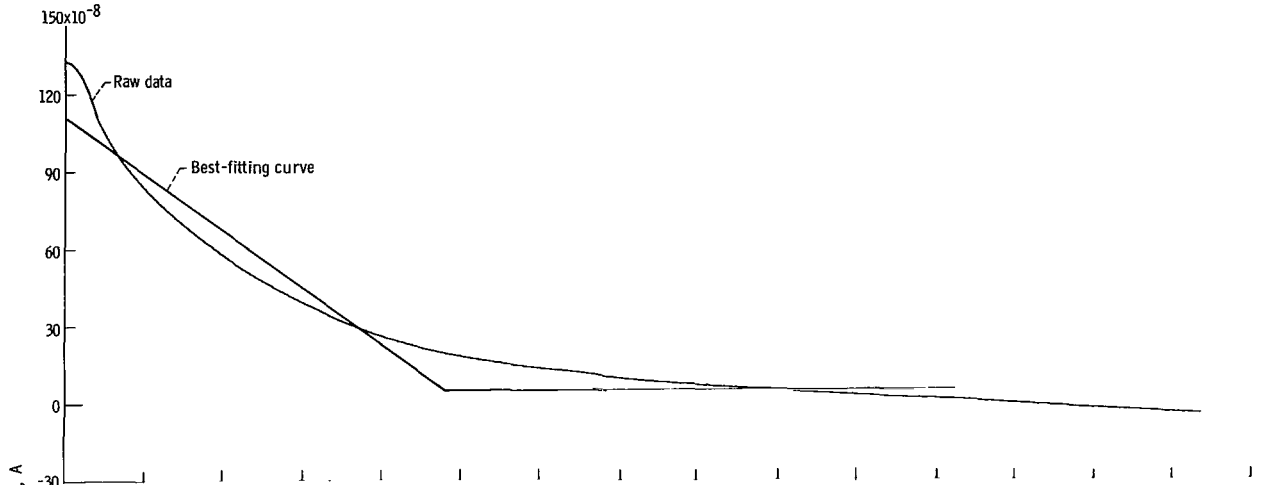

(c) Square-wave curve. Run AS-18; y-axis zero offset, I_0, 4.8×10^{-8} amperes; total particle flux reaching analyzer, I_1, 122×10^{-8} amperes; kinetic temperature, V_0, 550 electron volts per ion; floating potential, V_1, -142 volts; mean square error, 5.6 percent.

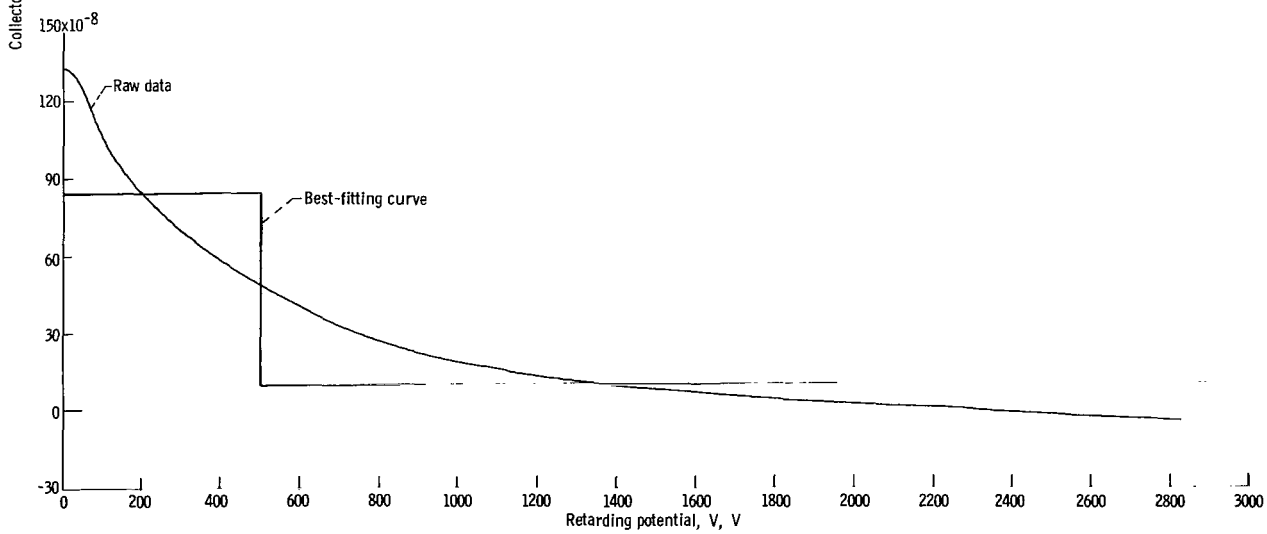

(d) Delta function curve. Run AS-24; y-axis zero offset, I_0, 9.7×10^{-8} amperes; total particle flux reaching analyzer, I_1, 74.1×10^{-8} amperes; kinetic temperature, V_0, 500 electron volts per ion; mean square error, 12.6 percent.

Figure 9. - Concluded.

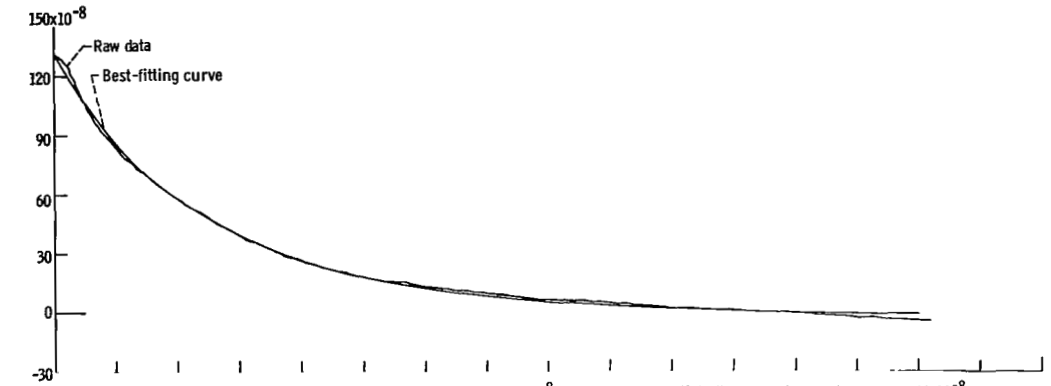

(a) Series AS. Run AS-22; pulsed fit; y-axis zero offset, I_0, -2.0×10^{-8} amperes; total particle flux reaching analyzer, I_1, 366×10^{-8} amperes; kinetic temperature, V_0, 710 electron volts per ion; floating potential, V_1, -308 volts; effective escape cone angle in velocity space, θ_0, 88°; mean square error, 1.11 percent.

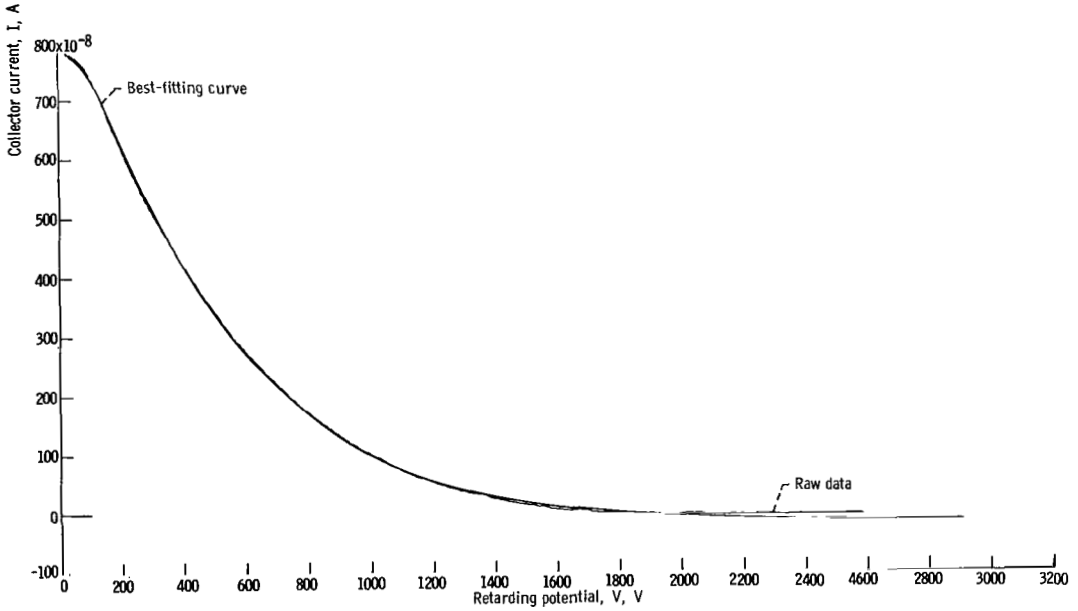

(b) Series AT. Run AT-1; pulsed fit; y-axis zero offset, I_0, -18×10^{-8} amperes; total particle flux reaching analyzer, I_1, 792×10^{-8} amperes; kinetic temperature, V_0, 464 electron volts per ion; floating potential, V_1, 33 volts; effective escape cone angle in velocity space, θ_0, 41°; mean square error, 0.53 percent.

Figure 10. - Best-fitting curves from each series.

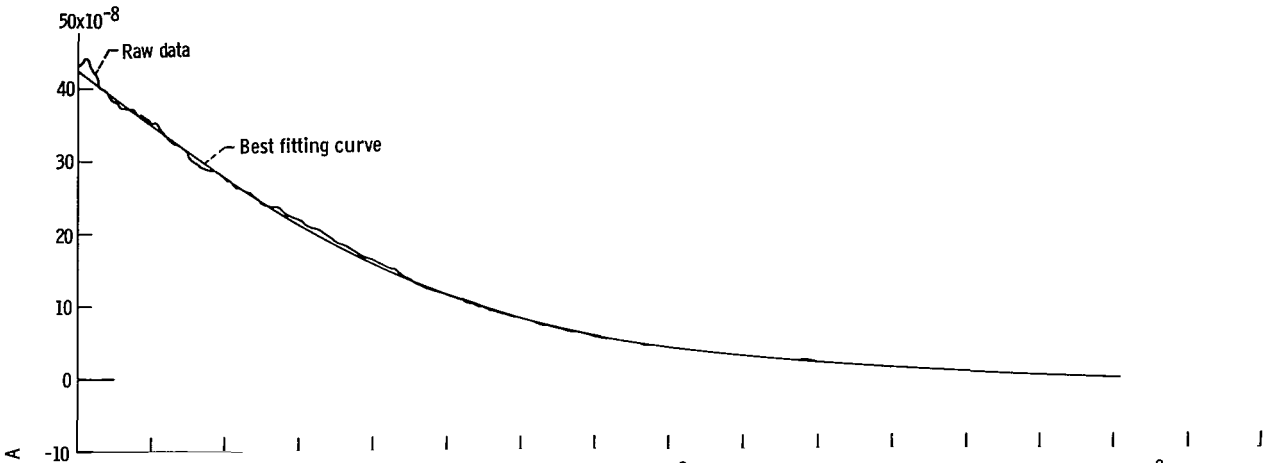

(c) Series AU. Run AU-15; steady fit; y-axis zero offset, I_0, -0.83×10^{-8} ampere; total particle flux reaching analyzer, I_1, 48×10^{-8} amperes; kinetic temperature, V_0, 620 electron volts per ion; floating potential, V_1, -237 volts; effective escape cone angle in velocity space, θ_0, 45°; mean square error, 0.79 percent.

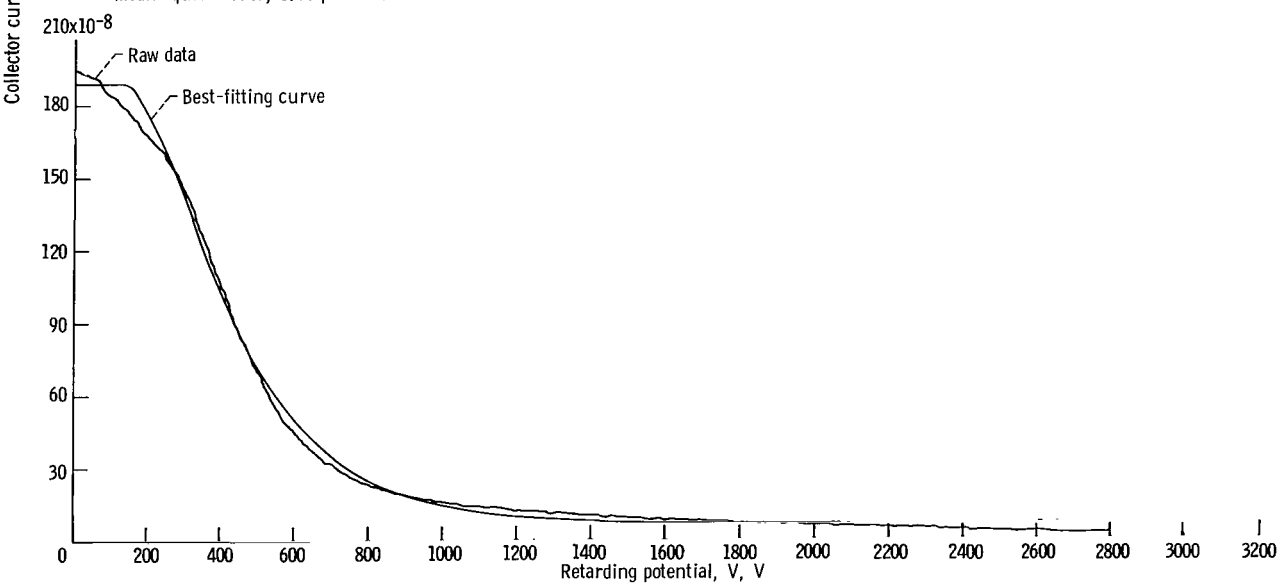

(d) Series AV. Run AV-1; steady fit; y-axis zero offset, I_0, 6.5×10^{-8} amperes; total particle flux reaching analyzer, I_1, 181×10^{-8} amperes; kinetic temperature, V_0, 196 electron volts per ion; floating potential, V_1, 126 volts; effective escape cone angle in velocity space, θ_0, 29°; mean square error, 1.68 percent.

Figure 10. - Concluded.

Sources of Error for Individual Runs

It is of interest to examine the possible sources of random and systematic error for an individual run and thereby place limits on the possible accuracy of this method of data analysis. The illustrative data already presented can be used as a framework for a discussion of various sources of error, as limitations on the precision of the calculated values, and of limitations on the physical models used in the interpretation of the data. Even the best-fitting curves exhibit some mean square error. This can result from three general sources: (1) the laboratory situation does not conform in all details to the theoretical model, (2) the measurements themselves have accuracy limitations and are not simultaneous, and (3) the sampling of the curves for computer processing is not completely representative.

Errors of the first kind include the following effects:

(1a) The distribution function of the ions in the discharge might not be Maxwellian along a radius within the escape cone in velocity space. Although one would expect this distribution from second law considerations (it is the most probable steady-state distribution), it is not a priori obvious that the ions in the discharge are confined long enough to equilibrate and become Maxwellianized.

(1b) The ion velocity distribution may not be isotropically distributed within the escape cone, or there might not be a sharp cutoff of number density at the effective escape cone angle. This situation can arise in the presence of nonadiabatic effects and an electric field between the plasma source and energy analyzer. This source of error may have contributed significantly to the lack of accuracy in determining the escape cone angle, and hence the term "effective" escape cone angle has been introduced.

(1c) The analytical curves with which the raw data curves are compared assume that the output of particles is either sharply pulsed or constant in time. A pulsed output with pulses of broad half width, or a rapid succession of smeared out pulses would result in an intermediate type of integrated energy spectrum and complicate the interpretation of the data.

(1d) In the present experiment, it was not expedient to aline the axis of the energy analyzer along the local magnetic field lines. These lines were at an angle of about 30^{o} with respect to each other under the experimental conditions, and this certainly introduced a systematic error into the calculation of the escape cone angle θ_{o}. It also would have made the velocity distribution asymmetrical about the analyzer axis, and this may have had a small effect on I_{1}, V_{o}, and the other parameters. Such an effect, however, should have been small by comparison with the other systematic and random errors present in this experiment. If a more accurate value of θ_{o} were desired, it would suffice to design the apparatus so that the analyzer axis is alined with the magnetic field lines. Such alinement was deemed not essential in the present series of experiments, since it

was desired only to show that the computer program could repeatably converge to the same value of θ_o, and that the influence on the curve shape of a particular θ_o could be reliably distinguished from small random run-to-run variations in the curve shape. An examination of tables III to VI reveals that the computer program did, in fact, reliably converge to a given escape cone angle, with a rather small mean error.

The magnitude of the curve-fitting error associated with the preceding four factors, individually or collectively, is difficult to estimate. Without calculating the retarding potential curve to be expected for individual anisotropic, non-Maxwellian models, there is no basis for comparison with the models used. The four models used as a basis for the computer program predict retarding potential curves of four distinct types. However, the reverse is not true - a curve of a given type might be obtained from some model that was not considered, or was intermediate among those considered.

Systematic errors introduced by the experimental apparatus include the following:

(2a) The discharge conditions may vary in time during an experimental run. This is a potentially serious source of error with this apparatus, since an individual X-Y plot required from 1 to 2 minutes, and the discharge conditions could not be kept absolutely constant over this duration. An inspection of figures 9(b), 10(a), 10(c), and 10(d) shows that the raw data curve performs small undulations about the best-fitting computer-derived curve. A retrace of the raw data (two successive runs traced on the same piece of graph paper) showed that at least part of this undulation can be attributed to time variation of the discharge characteristics while the retarding potential curve was being swept out.

(2b) The problems arising from analyzer design, including Debye sheaths, secondary electron emission, focusing effects, etc., have been treated extensively in the literature cited and are not discussed herein. Precautions were taken in the design of the present analyzer experiment to avoid the most obvious of such difficulties, and it is felt (based on the very low mean square error achieved in the series AT runs) that errors introduced by the analyzer design did not contribute significantly to the discrepancy between the analytical curves and the experimental data.

(2c) A small error may have been introduced into the data by time drift of the electronics during a run. All the apparatus was turned on to warm up at least 3 hours before a series of runs was taken. The variation during a given run was observed to occur only in the zero setting of the Y-axis of the recorder (i.e., I_o), and this was no more than about 0.5 percent of I_1.

(2d) The accuracy with which V_o can be determined in a given run depends on the accuracy with which the X-axis of the recorder was calibrated. In the present series of experiments, the retarding potential was measured with a 1-percent voltmeter, and the X-axis checked against this standard. The X-axis deflection agreed with the meter reading to within 1 percent. Table IV(b) shows that all the runs of the pulsed fit of the AT series had a mean square error of about 0.5 percent. This was the best fit of the four run

series studied. Since an additional inaccuracy of about 1 percent may have been introduced by the X-axis calibration, it is probably fair to conclude that the best possible accuracy with which the effective ion kinetic temperature can be determined is about 1.5 percent with the equipment used in the present experiment. The mean square errors obtained during the test runs could in some cases all be assigned to these relatively minor factors.

In addition to these errors, the computer processing involves the following additional factors:

(3a) Some error could be introduced into the data reduction procedure during the process of reading off the X-Y plots and listing evenly spaced data points in tabular form. Two different individuals could read the value of collector current (for a particular value of the retarding potential V) and obtain values that differed by no more than about 0.5 percent of the value of I_1. The errors introduced in tabulating the data and in keypunching it for use in the computer program are generally so gross that they are readily detected through their production of an anomalously high mean square error in the curve fit.

(3b) The computer program has been tested and refined through about 1500 curve fittings to the point where it will converge to a best-fitting curve for any integrated energy spectrum of monotonically decreasing form in more than 99 cases out of 100. No tendency has been observed of the program to exhibit bistable behavior, in the sense of converging to significantly different values of I_1, V_o, V_1, θ_o, and I_o for two closely similar raw data curves. As one may see from inspection of tables III to VI, only small differences in these parameters result from the small run-to-run variations that occur during a series of runs. It is always necessary, of course, to keep in mind the fact that a best fit to the experimental curve is not necessarily a good fit.

Sources of Error for a Series of Runs

One may obtain a useful idea of the precision of this method and of the run-to-run variations occurring under typical laboratory conditions by inspecting tables III to VII. The second last row of tables III to VI is the numerical average of the best-fitting parameters in that column, and the last row contains the mean error of this parameter, calculated by averaging the absolute values of the differences between the average value and the values for the individual runs. A comparison of the mean error with the average value may be used as a means of estimating the run-to-run variation. In table VII is shown the ratio of the mean error to the average value for the four run series considered and for the four theoretical distribution functions considered.

An examination of table VII shows that during run series AS and AT, the background

TABLE VII. - SUMMARY OF RUN-TO-RUN PERCENTAGE ERRORS

Run series	$\frac{\sum^{N} \lvert\Delta I_o\rvert}{N\bar{I}_o}$, percent	$\frac{\sum^{N} \lvert\Delta I_1\rvert}{N\bar{I}_o}$, percent	$\frac{\sum^{N} \lvert\Delta V_o\rvert}{N\bar{V}_o}$, percent	$\frac{\sum^{N} \lvert\Delta V_1\rvert}{N\bar{V}_1}$, percent	$\frac{\sum^{N} \lvert\Delta\theta_o\rvert}{N\bar{\theta}_o}$, percent	$\frac{\sum^{N} \lvert\Delta_{error}\rvert}{N_{error}}$, percent	$\frac{\sum^{N} \lvert\Delta p_T\rvert}{\bar{p}_T}$, percent	Remarks
Steady								
AS	60	7.5	1.4	5.6	6.7	7	0.9	
AT	20	2.3	5.9	18	4.8	7.2	.4	
AU	30	8.0	6.0	32	13	29	12	Best fit
AV	8.3	2.8	5.8	3.7	11	4.1	11	Best fit
Pulsed								
AS	21.5	13.9	1.4	9.2	7.5	11.4	----	Best fit
AT	15	2.1	5.2	15	2.5	15	----	Best fit
AU	24	7.5	5.2	52	12	29	----	
AV	9.4	2.8	5.7	2.3	11	3.2	----	
Square wave								
AS	7.35	0.9	3	18.3	----	1.25	----	
AT	5.2	.14	1.7	48	----	1.1	----	
AU	9	1.2	14	80	----	5.1	----	
AV	8.5	3.2	6.1	88	----	3.6	----	
Delta function								
AS	4.35	2.3	1.8	----	----	0.8	----	
AT	5.5	1.4	2	----	----	.7	----	
AU	5.4	11	5.9	----	----	2.3	----	
AV	6.6	2.8	5.9	----	----	2.8	----	

pressure varied by less than 1 percent of its mean value from run to run, while during run series AU and AV, the background pressure varied by about 12 percent. It is of some interest to see whether the rather large variation of background pressure might have been partly or mostly responsible for the run-to-run variations of V_o, V_1, I_1, θ_o, and I_o. In figures 11 and 12 are shown the parameters I_1 and V_o plotted as functions of the background vacuum tank pressure for a steady curve fit to the series AV runs. It is clear in this case that increasing values of V_o and I_1 are correlated with larger background pressures, although significant run-to-run variations still remain when the effects of changing pressure are accounted for. Figures 13 and 14 are similar plots for the AU run series, in which increasing values of vacuum tank pressure are associated with increasing values of the total collector current I_1, but decreasing values of plasma

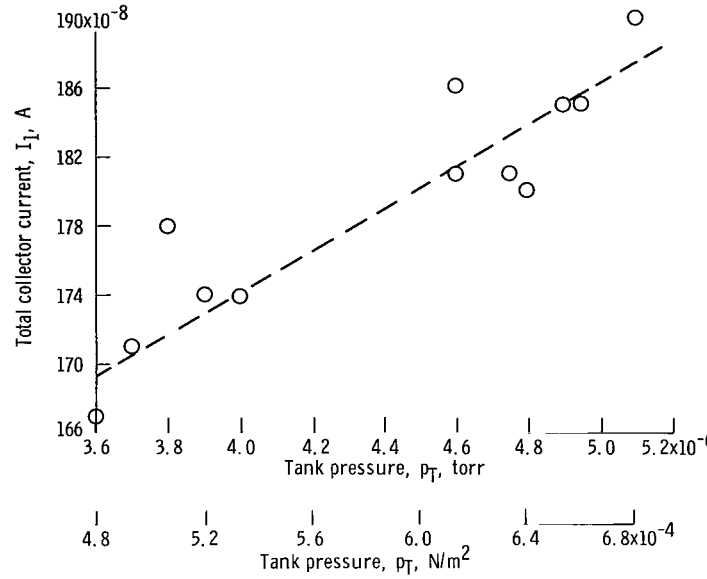

Figure 11. - Total particle flux reaching analyzer as function of vacuum tank pressure. Series AV; steady fit; expanded scale.

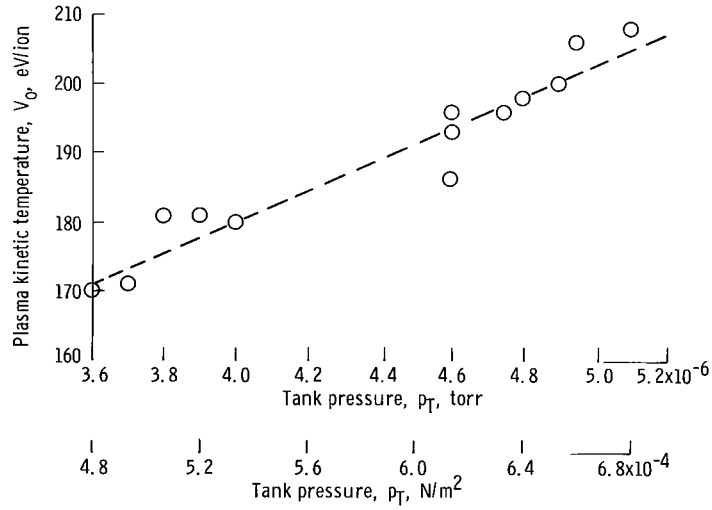

Figure 12. - Kinetic temperature as function of vacuum tank pressure. Series AV; steady fit; expanded scale.

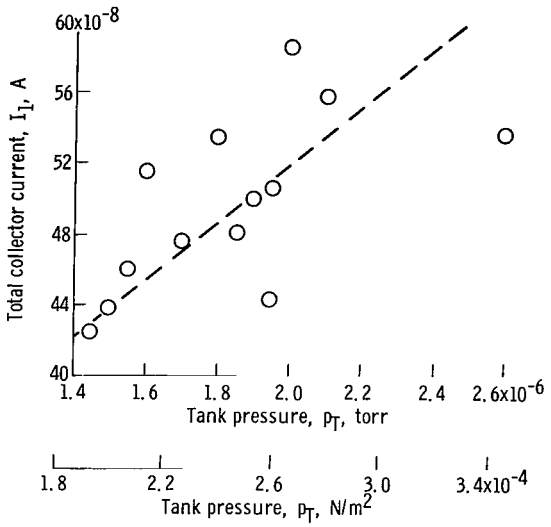

Figure 13. - Total particle flux reaching analyzer as function of vacuum tank pressure. Series AU; steady fit; expanded scale.

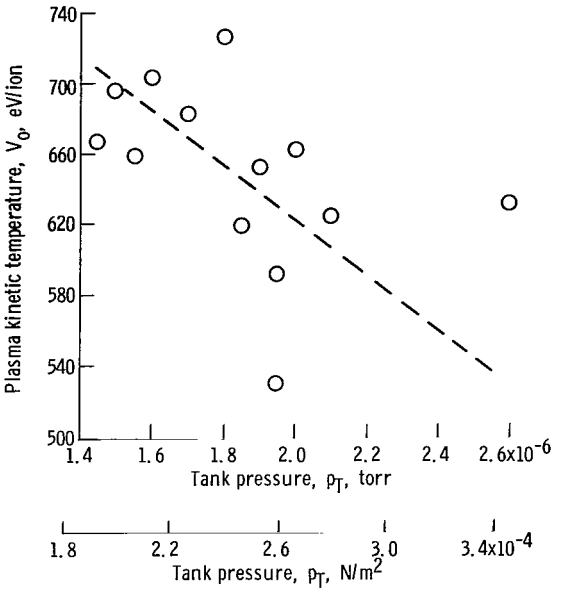

Figure 14. - Kinetic temperature as function of vacuum tank pressure. Series AV; steady fit; expanded scale.

kinetic temperature V_0. As in the AV run series, some, but not all, of the run-to-run variations can be ascribed to the uncontrollable changes of vacuum tank pressure in this apparatus.

An examination of table VII shows that the run-to-run variation in V_0, V_1, and I_1 of the AT run series is as great as that of the AU and AV series, even though the background pressure variation was much smaller than that of the latter two runs. An examination of table IV shows no systematic variation of I_1 or V_0 with the small variations of background pressure that did occur. One must look elsewhere for an explanation of the variations of the AT series. In figure 15 the parameters V_0 and I_1 are plotted as functions of the elapsed time at which the individual runs of the AT series were taken. There is an obvious similarity of the curves, which justifies the conclusion that much of the run-to-run variation in this series was the result of a time-dependent "hidden variable," which was some unmeasured characteristic of the discharge or apparatus other than the background pressure.

The run-to-run variation of the AS series apparently represents the best possible operating conditions with the lowest systematic error. The best-fitting parameters do not show any systematic trends with the small fluctuations in background pressure. Figures 16 and 17 show that the parameters V_0 and I_1 exhibit no systematic variation in time. Hidden variables are apparently not responsible for any time-dependent systematic errors, and therefore it is probably justified to conclude that the systematic errors in the

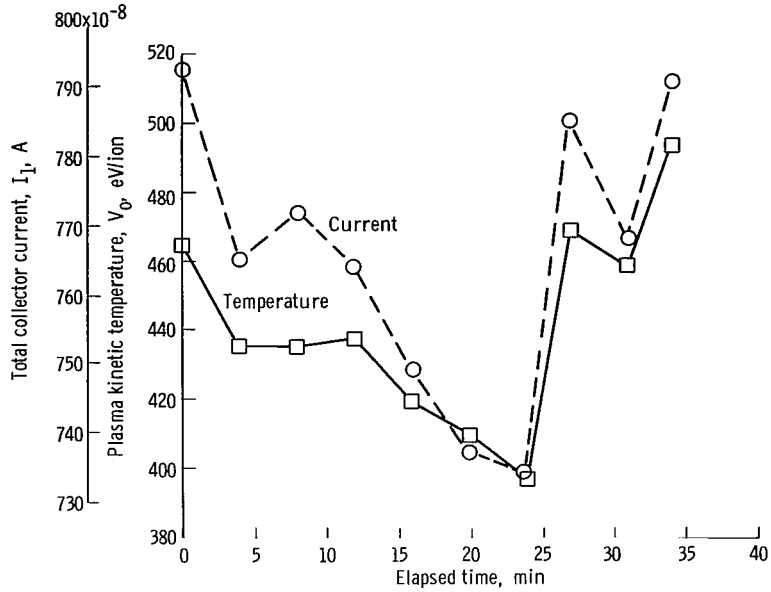

Figure 15. - Total particle flux reaching analyzer and kinetic temperature as functions of elapsed time. Series AT; pulsed fit.

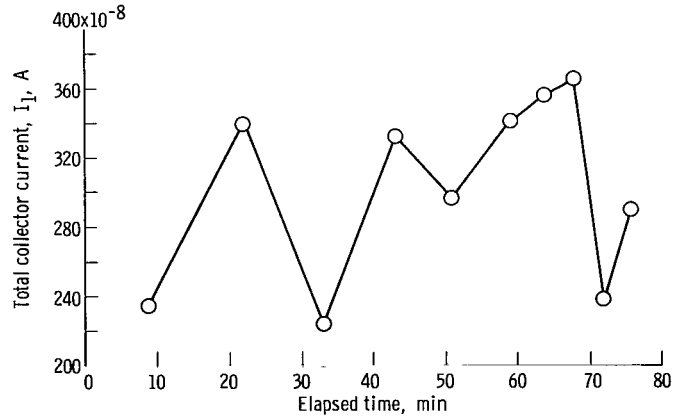

Figure 16. - Total particle flux reaching analyzer as function of elapsed time. Series AS; pulsed fit; expanded scale.

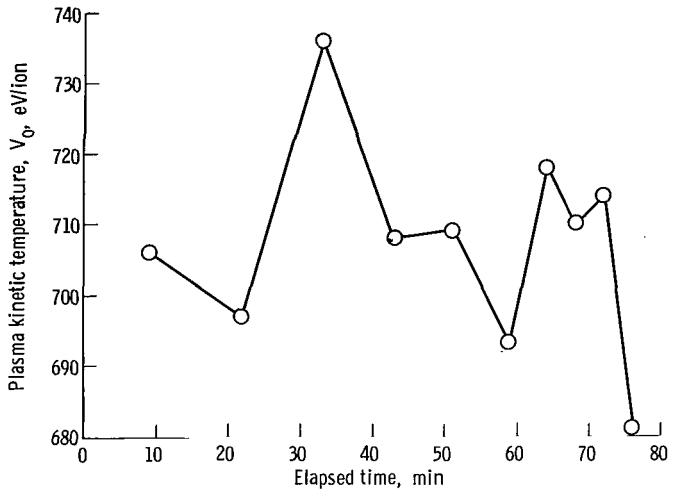

Figure 17. - Kinetic temperature as function of elapsed time. Series AS; pulsed fit; expanded scale.

AS series were as small as possible with this apparatus. If it is assumed that the AS run series had no systematic variation whatever attributable to the apparatus and that all the run-to-run variation for this series could be ascribed to imprecision of the data handling method described in this report, an upper limit can then be placed on the precision of this method.

The pulsed fit to the data of the AS run series (which was the best-fitting curve type) shows that the effective ion kinetic temperature had a run-to-run variation of only 1.4 percent, which compares favorably with other methods of determining this quantity. The floating potential V_1 was determined with a run-to-run variation of 9 percent, and the effective escape cone angle θ_0 varied by 7.5 percent. The parameter I_1 is proportional to the plasma density in the discharge and varied by 14 percent during the AS run series. This variation was larger than that of the other three run series. Even this large variation, however, compares favorably with the precision of Langmuir probe measurements of particle density made under similar conditions.

If the measurements described herein are typical of laboratory measurements in general, an examination of table VII suggests that it is reasonable to expect this method to yield a run-to-run variation of about 5 percent of the particle energy; 20 percent of the floating potential; 6 percent of I_1, and hence relative measurements of the charged particle density; and 10 percent of the value of the effective escape cone angle.

Discriminatory Ability of Data Analysis Technique

The reader has no doubt observed that run series AS and AT yielded a better fit to the pulsed integrated energy spectrum than to the integrated energy spectrum appropriate to a steady distribution of Maxwellian particles at the analyzer. An examination of tables III and IV shows that the pulsed fit was the better one in every run of these two series, and that the pulsed mean square error was substantially smaller than that of the steady curve fit in each run. This state of affairs appears very surprising in a steady-state experimental situation and requires comment.

An oscilloscope trace of the collector current is displayed in figure 18 as a function of time for three typical but distinct operating conditions. The time base in all three cases is 20 microseconds per centimeter, and the zero line is the base line between pulses. Figure 18(a) was taken under discharge operating conditions similar to those of run series AS and AT, and the ions are indeed reaching the collector in pulses. It is a peculiar characteristic of this discharge that particles are lost from it in periodic bursts under a wide variety of operating conditions. The pulses occur with a periodic frequency that has been analyzed and reported elsewhere (refs. 22 and 23).

Figure 18(b) shows the waveform of the current to the collector under intermediate operating conditions in which the pulse width is broader than the time of flight across the discharge, and the pulses are closer together in time. Figure 18(c) shows the collector current waveform under discharge operating conditions typical of run series AU and AV. The zero level is defined by the lowest excursion of the signal in this case. This waveform is above its zero level most of the time, but it does have individual peaks above the constant background current. The current waveform therefore has characteristics of both pulsed and steady-state operation. The steady and pulsed integrated energy spectra are about equally good fits to the raw data in run series AU and AV, as may be seen by examining the mean square errors for the individual runs of these series in tables V and VI. In contrast, the pulsed curve fit was unquestionably the better fit in series AS and AT, where the current waveform was clearly pulsed in nature.

The ability of the computer program to converge on the pulsed distribution, in a situation in which one might have expected the steady-state distribution to be appropriate, is an encouraging indication that it is possible to use the raw data to discriminate correctly among the possible energy distribution functions.

Large changes in the effective escape cone angle will result in only relatively small alterations in the geometric shape of the integrated energy spectrum. It is therefore proper to ask whether systematic variations in the escape cone angle can be discriminated from noise, run-to-run variations, or changes in the shape of the energy distribution function due to changes in the other discharge characteristics. Two series of runs (designated CK-CL and CM-CN) were made to indicate (but not prove) that such discrim-

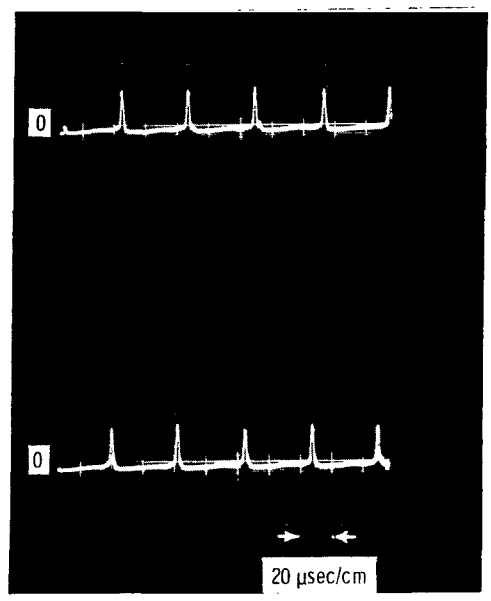

(a) Low density; high ion energy.

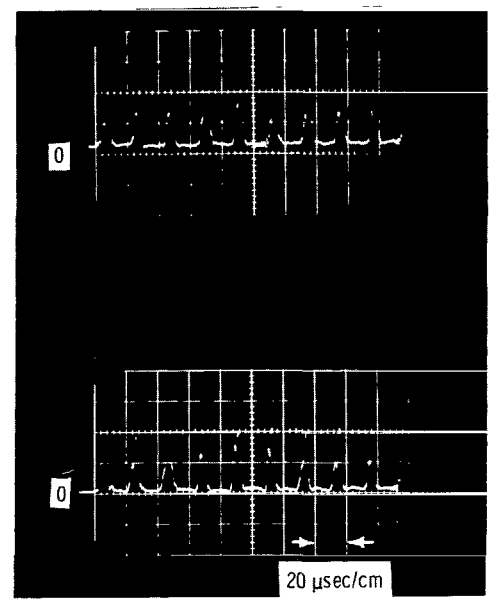

(b) Intermediate densities and ion energies.

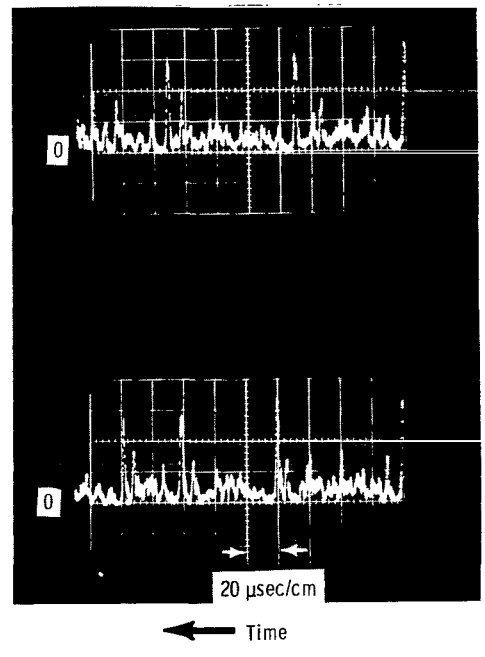

(c) High densities; low ion energies.

Figure 18. - Collector current as function of time.

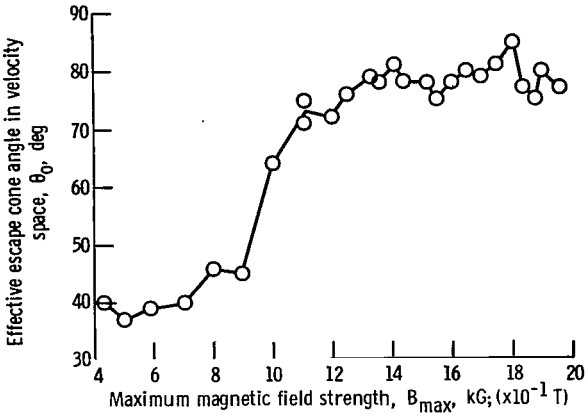

Figure 19. - Effective escape cone angle as function of magnetic field strength. Run series CK-CL.

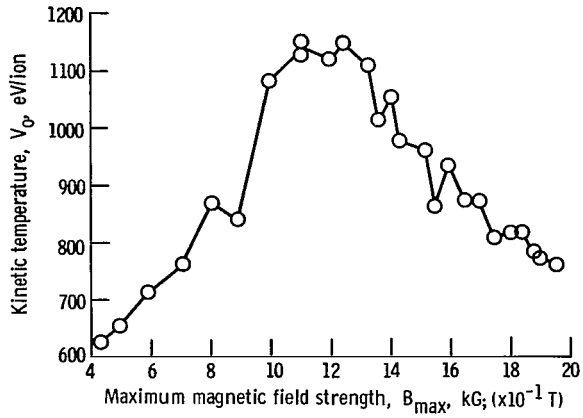

Figure 20. - Kinetic temperature as function of maximum magnetic field strength. Run series CK-CL.

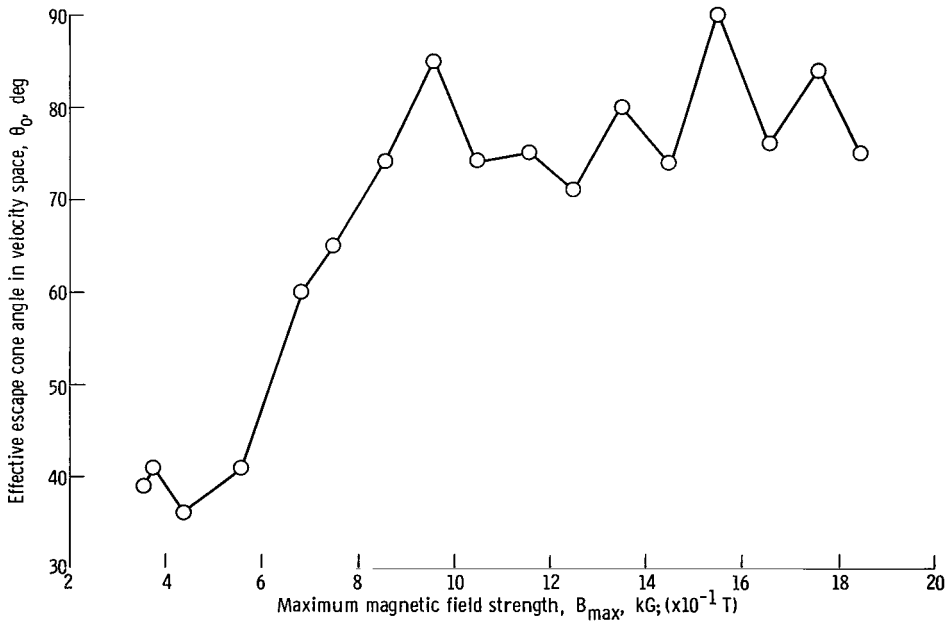

Figure 21. - Effective escape cone angle as function of maximum magnetic field strength. Run series CM-CN.

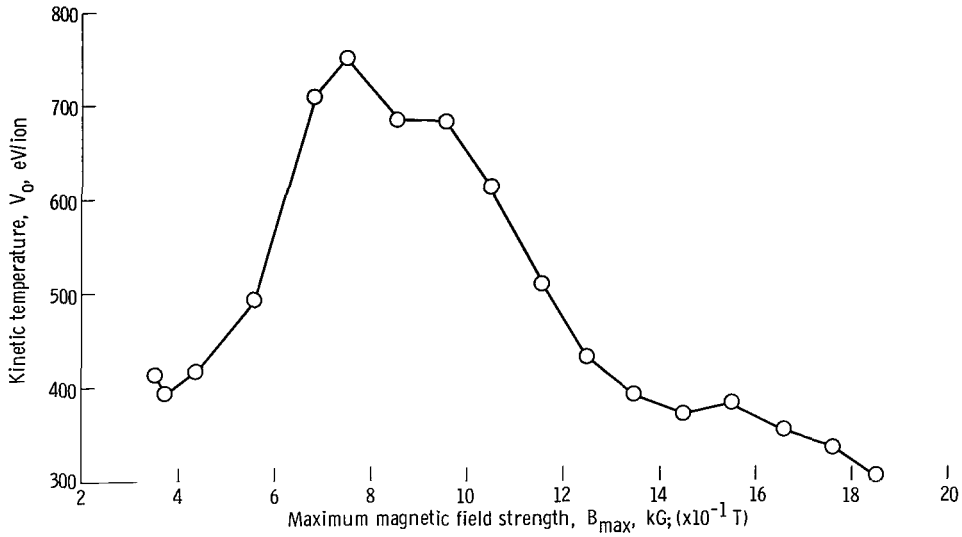

Figure 22. - Kinetic temperature as function of maximum magnetic field strength. Run series CM-CN.

ination in the effective escape cone angle is possible under laboratory conditions.

The individual runs in these series were made at different magnetic field strengths, while all other discharge parameters shown in table II remained the same. The results are plotted in figures 19 to 22. Figures 19 and 21 show the best-fitting effective escape cone angle plotted as a function of magnetic field strength. There is clearly a systematic trend in the data of increasing escape cone angle with increasing magnetic field strength. The run-to-run variation of θ_o about a smooth curve through the data points is approximately the ±10 percent variation that the four earlier run series led one to expect. The ion kinetic temperature is plotted as a function of magnetic field strength on figures 20 and 22. A systematic trend is evident here also. The kinetic temperature and escape cone angle increase together to the point at which the kinetic temperature is a maximum, after which the kinetic temperature decreases and the effective escape cone angle is constant with magnetic field strength.

An interpretation of these data in terms of processes occurring in the discharge is beyond the scope of this report. The increase of escape cone angle with magnetic field shown in figures 19 and 21 is surprising. However, qualitatively similar behavior was observed in the two run series CK-CL and CM-CN, which were taken under different discharge operating conditions, and this is considered to reinforce the contention that figures 19 to 22 show the actual behavior of the parameters indicated.

CONCLUSIONS

Analytical expressions have been derived for the integrated energy spectra which result from a pulsed and steady-state flux of Maxwellianized particles. These energy spectra include as parameters the floating potential V_1 of the source of the particles, the kinetic temperature V_o of the particles, and the half-angle θ_o of the cone which they occupy in velocity space. A computer program was written which obtains best-fitting values of these parameters for a given experimental energy spectrum. The raw data from a series of experimental runs with a retarding potential energy analyzer were compared with these analytical expressions by this computer program, and the best-fitting values of V_o, V_1, and θ_o obtained for the experimental conditions.

Certain series of runs were best fitted by the integrated energy distribution function appropriate to a pulsed output of particles. This result, rather surprising in the "steady-state" discharge under investigation, was consistent with the results of additional investigation. The dynamics of the discharge were such that particles were, in fact, reaching the energy analyzer in pulses.

Four series of at least 10 individual runs were made to obtain typical values of the run-to-run variation to be expected by using this technique. Each of the four series was held under conditions as nearly constant as the experimental apparatus would allow. For the experiment used as an example, this data analysis technique typically yielded a run-to-run variation of about 5 percent of the particle kinetic temperature; 20 percent of the floating potential; 6 percent of I_1, and hence on relative measurements of the charged particle density; and 10 percent of the value of the effective escape cone angle.

Lewis Research Center,
National Aeronautics and Space Administration,
Cleveland, Ohio, April 8, 1968,
129-02-03-05-22.

APPENDIX A

NOMENCLATURE

Mathematical symbol	FORTRAN symbol	Description
A	---	area of energy probe aperture, m^2
B_{max}	---	maximum magnetic field, T (kG)
B_o	---	magnetic field existing at collector, T (kG)
e	---	electronic charge, 1.602×10^{-19} C
G	---	geometry factor
I_o	IA	y-axis zero offset on energy spectra curve
I_1	IB	total current to analyzer, defined by eq. (49)
i	---	current, A
i_1	---	total current, defined by eq. (28)
j	---	current density, A/m^2
k	---	Boltzmann constant, 1.38×10^{-23} $J/^oK$
N_o	---	number of particles emitted by source over hemisphere in velocity space, per pulse
n	---	particle number density, particles/m^3
n_o	---	particle number density of source, particles/m^3
T	---	kinetic temperature, ^oK
V_o	VA	particle kinetic temperature, eV
V_1	VB	floating potential of plasma, V
V_2	VC	potential defined in fig. 6(a), V
v	---	particle speed, m/sec
v_o	---	most probable speed, m/sec
v_z	---	particle velocity in z-direction, m/sec
v_{zo}	---	velocity defined by eq. (9), m/sec
$\bar{v}$	---	average speed of particles, $\sqrt{8\gamma RT/\pi M}$, m/sec

Mathematical symbol	FORTRAN symbol	Description
W	---	number of particle pulses per second
x_0	---	dimensionless parameter defined by eq. (33)
θ	---	angle with respect to z-axis and/or magnetic field line
θ_o	TH	effective escape cone angle in velocity space
φ	---	rotational angle in plane normal to z-axis and/or magnetic field line

APPENDIX B

COMPUTER PROGRAM

by Loretta R. Ellis

A computer program was written to find values of the constants I_o, I_1, V_o, V_1, θ_o in four analytical expressions, such that a best-fitting curve is obtained. These expressions are given in equations (40) to (48). The least squares method was used for each curve fit. This method states that the best-fitting curve is that for which the sum of the squares of the residuals is a minimum. To use this method conveniently, the equations should be linear in the unknown constants. The given expressions are not of this form; therefore, new expressions were derived which were linear in corrections for approximate values of the constants.

According to Scarborough (ref. 24), this can be done as follows: Let $y = f(x, a, b)$ be a given function from expressions (40) to (48). Let a_o and b_o be approximate values of the unknown constants a and b, and let α and β denote corrections to a_o and b_o such that $a = a_o + \alpha$ and $b = b_o + \beta$. Then $y' = f(x, a_o, b_o)$ will be a function whose graph approximates the graph of $y = f(x, a, b)$. If the graph of $y = f(x, a, b)$ passes as near as possible to each of the n points (x_1, y_1), (x_2, y_2), . . ., (x_n, y_n) on the experimental curve, the residuals v_k will be the difference between the computed and observed values

$$v_k = f(x_k, a, b) - y_k \tag{B1}$$

or

$$v_k = f(x_k, a_o + \alpha, b_o + \beta) - y_k \tag{B2}$$

where $y_k = y(x_k)$ represents the k^{th} point on the experimental curve ($k = 1, 2, \ldots, n$). Using Taylor's expansion for a function of several variables, one obtains

$$f(x_k, a_o + \alpha, b_o + \beta) = f(x_k, a_o, b_o) + \alpha\left(\frac{\partial f}{\partial a}\right)_{\substack{a=a_o \\ b=b_o}} + \beta\left(\frac{\partial f}{\partial b}\right)_{\substack{a=a_o \\ b=b_o}} + \text{Higher order terms} \tag{B3}$$

Omitting the higher order terms gives equation (B1) in the form

$$v_k = f(x_k, a_o, b_o) + \alpha\left(\frac{\partial f}{\partial a}\right)_{\substack{a=a_o \\ b=b_o}} + \beta\left(\frac{\partial f}{\partial b}\right)_{\substack{a=a_o \\ b=b_o}} - y_k \tag{B4}$$

or

$$v_k = v'_k + \alpha\left(\frac{\partial f}{\partial a}\right)_{\substack{a=a_o \\ b=b_o}} + \beta\left(\frac{\partial f}{\partial b}\right)_{\substack{a=a_o \\ b=b_o}} - y_k \tag{B5}$$

Let $r_k = y'_k - y_k$, where r_k is the residual for the approximation curve $y'_k = f(x_k, a_o, b_o)$ since it is the difference between the observed ordinates and the ordinates of this curve. Then

$$v_k = \alpha\left(\frac{\partial f}{\partial a}\right)_{\substack{a=a_o \\ b=b_o}} + \beta\left(\frac{\partial f}{\partial b}\right)_{\substack{a=a_o \\ b=b_o}} + r_k \tag{B6}$$

The method of least squares can be applied now to find the corrections α and β, given approximate values a_o and b_o.

In finding the best representative curves for the four expressions, better results were obtained by solving for two constants at a time and holding the remaining constants fixed, rather than trying to solve for more than two constants. Those constants which were the hardest to approximate were the first on which to be iterated.

Initial values for the constants I_o, I_1, V_o, and V_1 are supplied by the user in the main program. The initial value of θ_o is taken as 40^o (θ_o is converted to radians for the computations). These initial values are used as approximate starting values in each of the four curve fits.

The main program SPECTR (fig. 23) reads the input data, supplies this information to the subprograms, stores the results until all the calculations are completed for a given set of data, then prints those results.

Subroutine MODE (fig. 24) finds the best-fitting values for the constants I_o, I_1, V_o, V_1, θ_o for the steady-state and for the pulsed-state expressions. Subroutines STEADY (fig. 25) and PULSED (fig. 26) supply the derivatives and residuals for those expressions for the least squares evaluation of the corrections needed (steps (1) and (2) following). Subroutine CALC (fig. 27) provides the necessary calculations for step (3). The iteration cycle consists of three steps:

(1) Maximum of five iterations to find V_o and V_1, keeping I_o, I_1, and θ_o fixed until the corrections are small enough

(2) Maximum of five iterations to find I_1 and θ_o, keeping I_o, V_o, and V_1 fixed until

(a) Corrections are small enough

(b) $|\Delta\theta_o| > 0.5$

(c) $(\theta_o + \Delta\theta_o)$ falls outside the range $(0, \pi/2)$

(3) Maximum of 50 iterations to find I_o keeping I_1, V_o, V_1, and θ_o fixed

The values of the constants are updated after each iteration. On completion of step (3), the values are compared with those supplied at the beginning of the cycle. If they do not agree within the limits specified, the preceeding three steps are repeated for a maximum of 50 cycles or until the values do agree to three significant places. The values at the end of a cycle become starting values at the beginning of the next cycle.

Subroutine SQUARE (fig. 28) finds the best fitting values for the constants I_o, I_1, V_o, and V_1 for the square wave function. The method used here is divided into two parts:

(1) Maximum of five iterations to find V_o and V_1, keeping I_o and I_1 fixed until the corrections are small enough

(2) Maximum of five iterations to find I_o and I_1, keeping V_o and V_1 fixed, until the corrections are small enough

The values of the constants are now compared with those from the beginning of the cycle. If they do not agree within the limits specified, the preceding two steps are repeated for a maximum of 50 cycles or until the values do agree to three significant places. As in MODE, the values at the end of one cycle become starting values at the beginning of the next cycle.

Subroutine FDELTA (fig. 29) finds the best-fitting values for the constants I_o, I_1, and V_o for the delta-wave function. Values of I_o and I_1 are found as V_o takes on successive values of V from the input curve. When the mean square error between the computed curve and the input curve reaches a minimum, the iteration stops. The maximum number of iterations is the same as the number of points on the given curve. Control is then returned to the main program for storage of output.

Subroutine LESQ (fig. 30) finds the normal equations according to the least squares method, given the necessary derivatives and residuals for each data point. It then uses these equations to solve for the unknowns. The normal equations here are two equations in two unknowns, the unknowns being the corrections.

Subroutine STEADY, PULSED, and CALC supply the necessary computations (derivatives, residuals, etc.,) for subroutine MODE.

The input consists of the following cards for each set of data:

(1) The first card contains the run number RUN, the number of points N for this

particular curve, and a control indicator NV. RUN is read in alphameric format; N and NV are read in integer format and both must be less than 100, the maximum size of the V- and I-arrays. These three values RUN, N, and NV, must end in card columns 5, 10, and 15, respectively.

(2) If $NV \leq 0$, the V-array is unchanged. If $NV > 0$, the first NV elements of the V-array are read. In order to minimize card input, the maximum number of elements needed of the V-array are read in, then left unchanged until new values are read again (when $NV > 0$). Hence, NV should be as large as the largest N which will be associated with it.

(3) Next, the first N elements of the I-array are read in.

The elements of the V- and I-arrays are read in floating-point format with 10 card columns allowed for each value. There are eight numbers per card. The last card of each array may have less than eight numbers on it.

(4) The last card of the input set contains the initial values for I_0, I_1, V_0, and V_1. The values are read in floating-point format with 10 card columns allowed for each value.

The program stops when there are no more data to be read. Sample input is included with the FORTRAN listing.

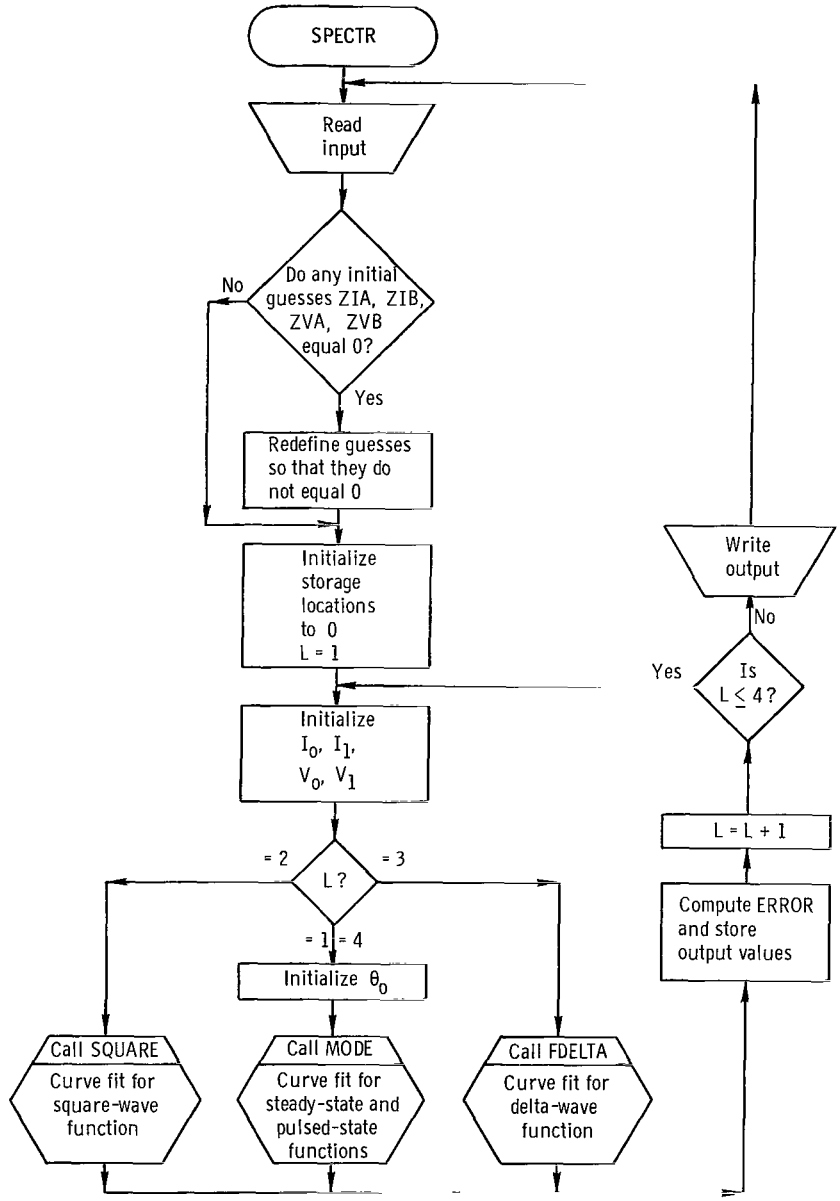

Figure 23. - Flow chart for main program SPECTR.

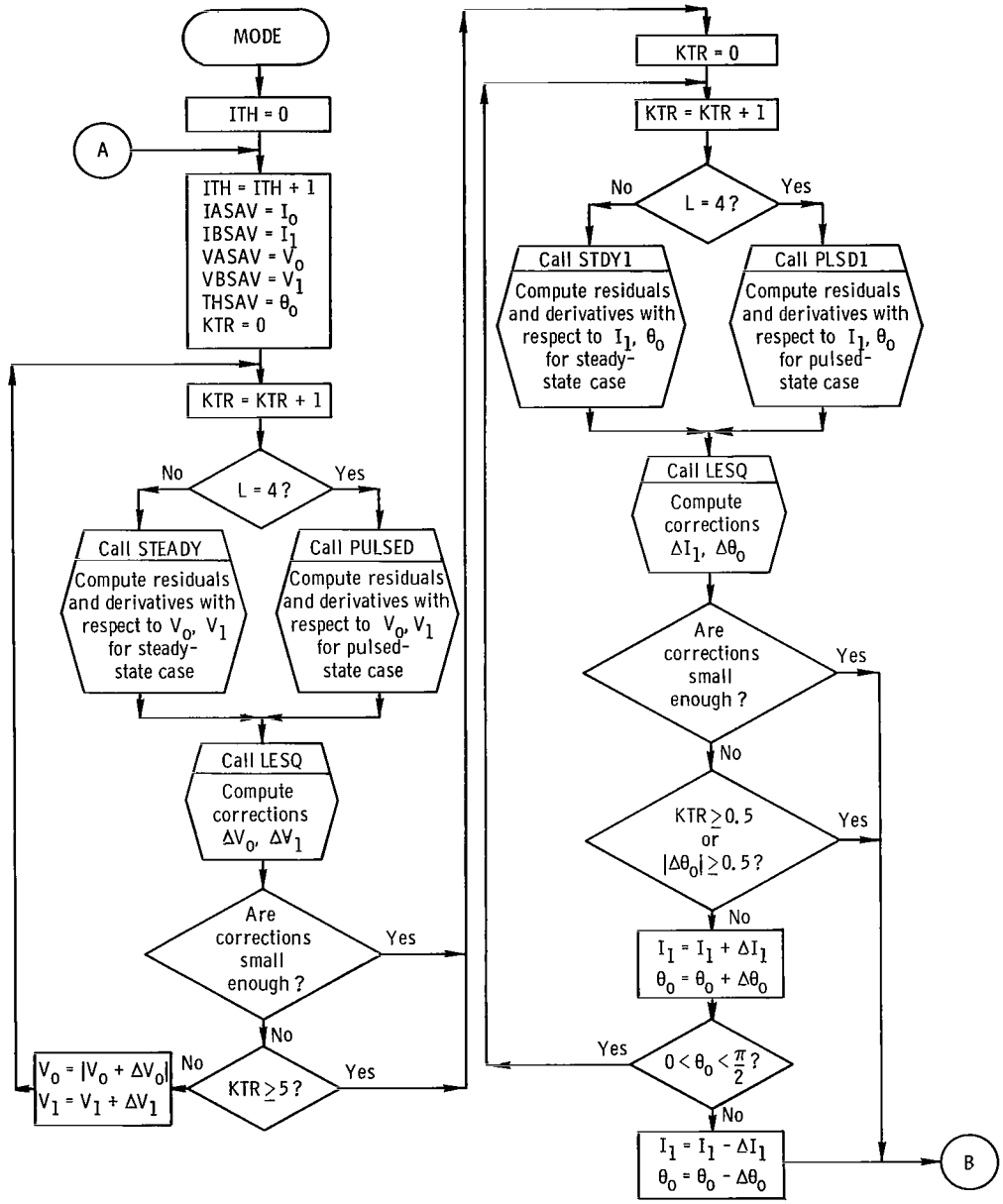

Figure 24. - Flow chart for subroutine MODE.

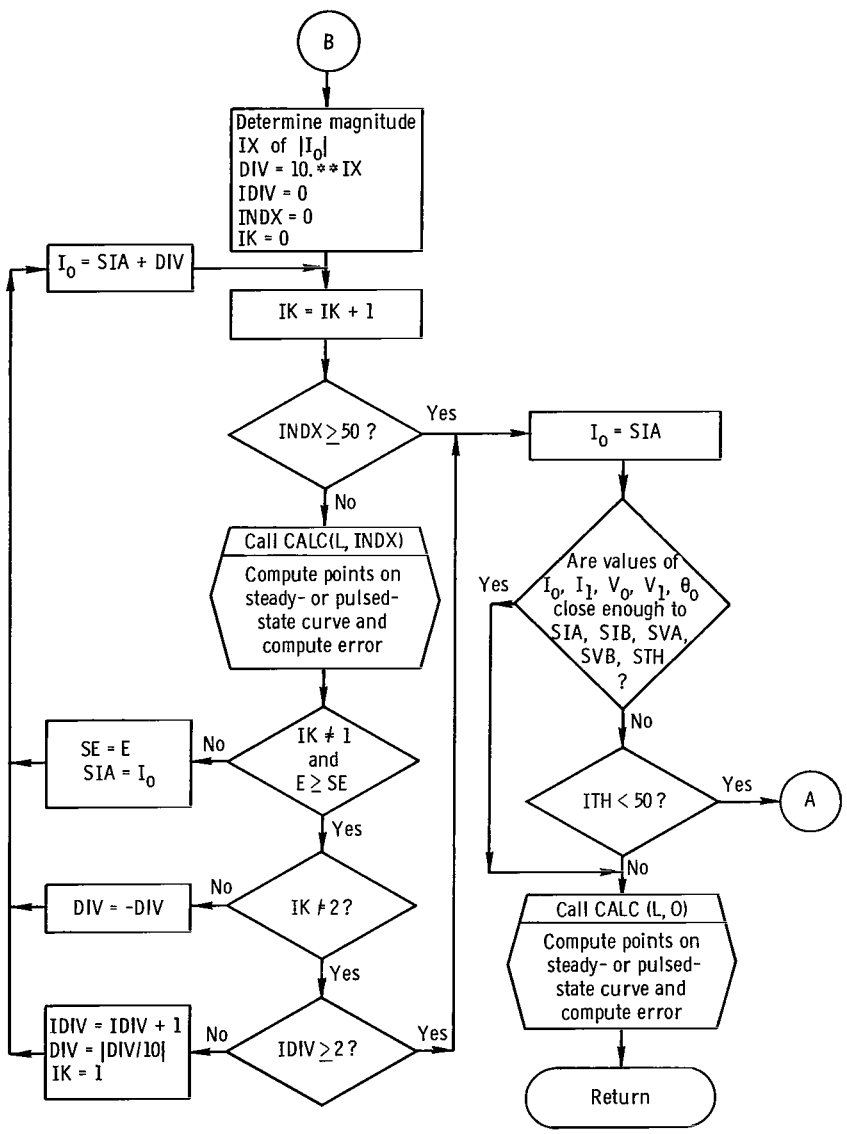

Figure 24. - Concluded.

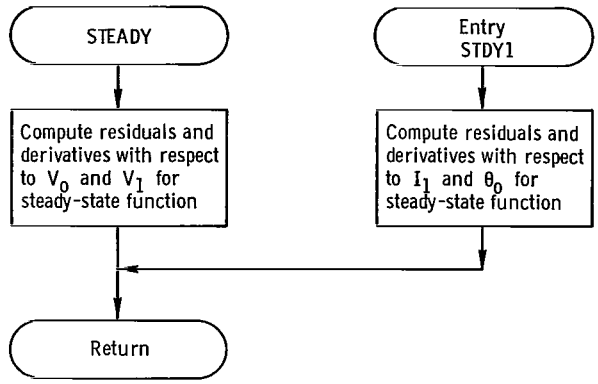

Figure 25. - Flow chart for subroutine STEADY.

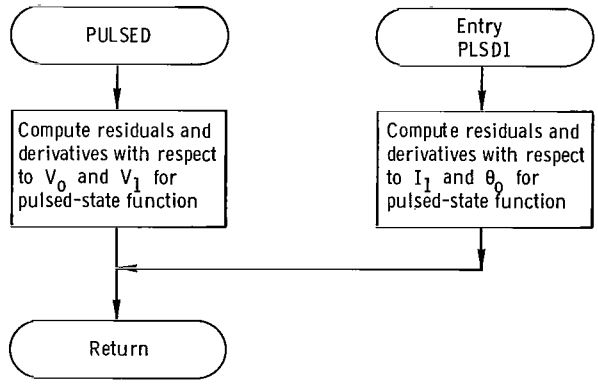

Figure 26. - Flow chart for subroutine PULSED.

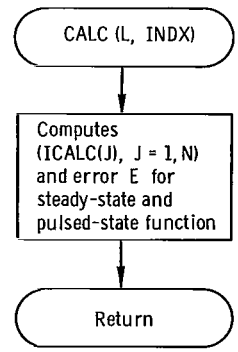

Figure 27. - Flow chart for subroutine CALC.

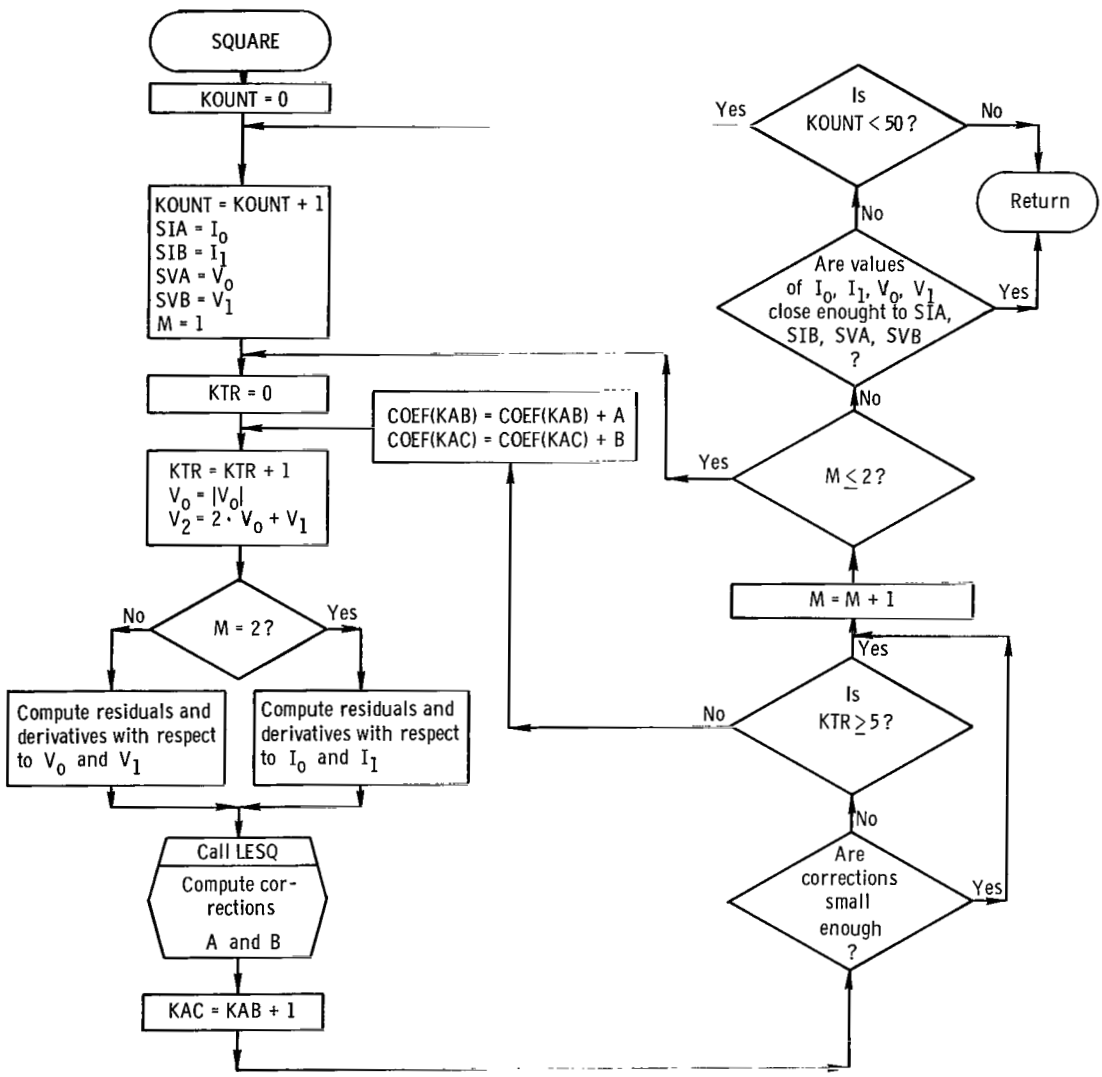

Figure 28. - Flow chart for subroutine SQUARE.

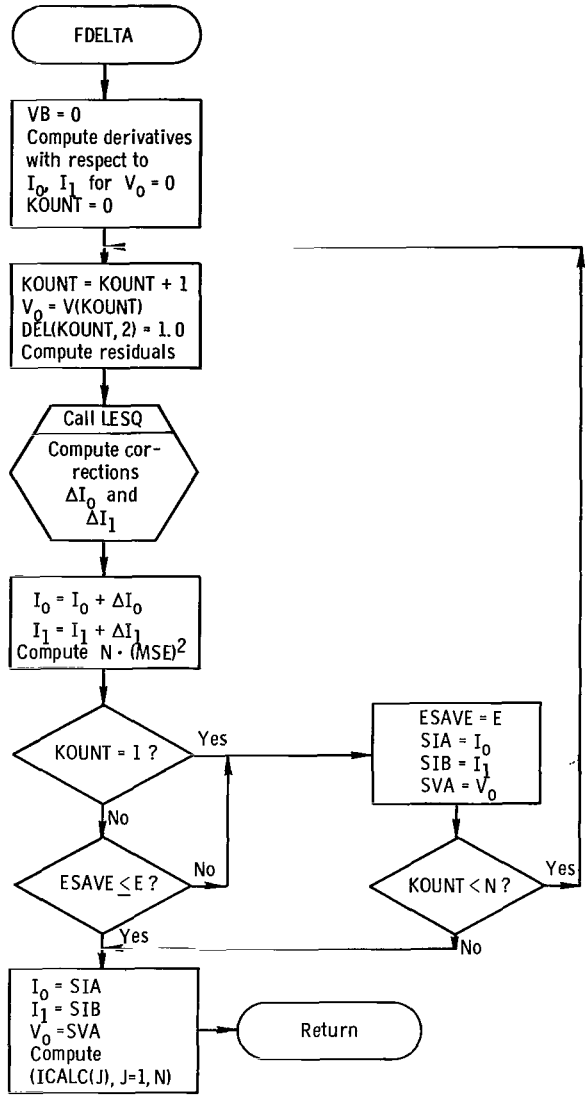

Figure 29. - Flow chart for subroutine FDELTA.

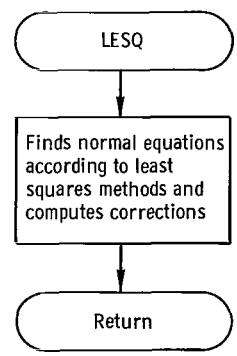

Figure 30. - Flow chart for subroutine LESQ.

```
$IBFTC SPECTR  LIST,DECK                                                    SPE  00
      DIMENSION COEF(5),ZI(100,5),Z(10,5),ZX(5),CO(5)                       SPE  10
      COMMON /ALL/N,V(100),I(100),ICALC(100),DEL(100,5),IA,IB,VA,           SPE  20
     1 VB,TH,A,B,E,M,KOUNT,KTR                                              SPE  30
      EQUIVALENCE (COEF(1),IA), (ZX(1),ZIA),(ZX(2),ZIB),(ZX(3),ZVA),        SPE  40
     1 (ZX(4),ZVB),(ZX(5),ZTH)                                              SPE  50
      EQUIVALENCE (CO(1),IASAV),(CO(2),IBSAV),(CO(3),VASAV),                SPE  60
     1 (CO(4),VBSAV),(CO(5),THSAV)                                          SPE  70
      REAL I,ICALC,IA,IB,IASAV,IBSAV                                        SPE  80
      DATA ZTH,ZZTH/40.,0.69813/                                            SPE  90
C                                                                           SPE 100
C     RUN IS THE RUN NUMBER                                                 SPE 110
C     (V,I) ARE THE (X,Y) COORDINATES - VOLTAGE VS CURRENT                  SPE 120
C     NONE OF THE INITIAL GUESSES ZIA,ZIB,ZVA,ZVB, SHOULD BE EQUAL TO ZESPE 130
C     N = NUMBER OF POINTS (V,I) - N.LE.100                                 SPE 140
C     NV = CONTROL INDICATOR                                                SPE 150
C        NV.LE.0  PREVIOUS VALUES OF V(J) ARE TO BE USED                    SPE 160
C        NV.GT.0  NV ELEMENTS OF V ARE TO BE USED...NV.GE.MAXIMUM N         SPE 170
C                 AND NV.LE.100                                             SPE 180
C     V(J)     VOLTAGE INPUT                                                SPE 190
C     I(J)     CURRENT INPUT                                                SPE 200
C     ZI(J,K) CALCULATED CURRENT USING FINAL VALUES OF IA,IB,VA,VB          SPE 210
C     Z(L,K)                                                                SPE 220
C        J=1,N           (DENOTES WHICH POINT)                              SPE 230
C        K=1,4           (K=1 DENOTES STEADY-STATE MODE)                    SPE 240
C                        (K=2 DENOTES SQUARE-WAVE FUNCTION)                 SPE 250
C                        (K=3 DENOTES DELTA FUNCTION)                       SPE 260
C                        (K=4 DENOTES PULSED MODE)                          SPE 270
C        L=1,10          (L=1 DENOTES IA (I(0)) )                           SPE 280
C                        (L=2 DENOTES IB (I(1)) )                           SPE 290
C                        (L=3 DENOTES VA (V(0)) )                           SPE 300
C                        (L=4 DENOTES VB (V(1)) )                           SPE 310
C                        (L=5 DENOTES THETA )                               SPE 320
C                        (L=6 DENOTES THE NUMBER OF ITERATIONS )            SPE 330
C                        (L=7 DENOTES THE MEAN SQUARE ERROR )               SPE 340
C                                                                           SPE 350
10    WRITE (6,90)                                                          SPE 360
      READ (5,100) RUN,N,NV                                                 SPE 370
      IF (NV.GT.0) READ (5,110) (V(J),J=1,NV)                               SPE 380
      READ (5,110) (I(J),J=1,N)                                             SPE 390
      READ (5,110) ZIA,ZIB,ZVA,ZVB                                          SPE 400
      IF (ZIA.EQ.0.0) ZIA=I(N)*0.001                                        SPE 410
      IF (ZIA.EQ.0.0) ZIA=1.0E-3                                            SPE 420
      IF (ZIB.EQ.0.0) ZIB=I(1)                                              SPE 430
      IF (ZVA.EQ.0.0) ZVA=V(2)                                              SPE 440
      IF (ZVB.EQ.0.0) ZVB=V(2)                                              SPE 450
      FLN=N                                                                 SPE 460
      DO 20 J=1,5                                                           SPE 470
      DO 20 K=1,10                                                          SPE 480
20    Z(K,J)=0.0                                                            SPE 490
      DO 80 L=1,4                                                           SPE 500
```

```
      IA=ZIA                                                                SPE 510
      IB=ZIB                                                                SPE 520
      VA=ZVA                                                                SPE 530
      VB=ZVB                                                                SPE 540
      GO TO (30,40,50,30),L                                                 SPE 550
30    TH=ZZTH                                                               SPE 560
      CALL MODE (L)                                                         SPE 570
      Z(5,L)=57.295779*TH                                                   SPE 580
      GO TO 60                                                              SPE 590
40    CALL SQUARE                                                           SPE 600
      GO TO 60                                                              SPE 610
50    CALL FDELTA                                                           SPE 620
60    S=0.0                                                                 SPE 630
      DO 70 J=1,N                                                           SPE 640
      ZI(J,L)=ICALC(J)                                                      SPE 650
70    S=S+(I(J)-ICALC(J))**2                                                SPE 660
      Z(1,L)=IA                                                             SPE 670
      Z(2,L)=IB                                                             SPE 680
      Z(3,L)=VA                                                             SPE 690
      Z(4,L)=VB                                                             SPE 700
      Z(6,L)=KOUNT                                                          SPE 710
      Z(8,L)=IB/ASQRT(VA)                                                   SPE 720
80    Z(7,L)=100./I(1)*SQRT(S/FLN)                                          SPE 730
      WRITE (6,120) RUN,(J,V(J),I(J),(ZI(J,L),L=1,4),J=1,N)                 SPE 740
      WRITE (6,130) (ZX(J),(Z(J,L),L=1,4),J=1,5),((Z(J,L),L=1,4),J=6,7)     SPE 750
      WRITE (6,140) (Z(8,L),L=1,4)                                          SPE 760
      GO TO 10                                                              SPE 770
C                                                                           SPE 780
C                                                                           SPE 790
C                                                                           SPE 800
90    FORMAT (1H1)                                                          SPE 810
100   FORMAT (A5,2I5)                                                       SPE 820
110   FORMAT (8E10.0)                                                       SPE 830
120   FORMAT (16H   RUN  NUMBER  ,A5/1HK,12X,1HV,15X,1HI,13X,6HSTEADY,10SPE 840
     1X,7HSQ-WAVE,9X,5HDELTA,11X,6HPULSED//(I5,F12.3,4X,5E16.5))           SPE 850
130   FORMAT (1HL//27X,7HINITIAL,9X,6HSTEADY,10X,7HSQ-WAVE,9X,5HDELTA,11SPE 860
     1X,7HPULSED //13X,8HI0 =     ,5E16.5/13X,8HI1 =     ,5E16.5/13X,8HV0 SPE 870
     2=     ,5E16.5/13X,8HV1 =     ,5E16.5/13X,8HTHETA = ,5E16.5//13X,8HKOSPE 880
     3UNT = ,16X,4E16.5/13X,8HERROR = ,16X,4E16.5)                          SPE 890
140   FORMAT (13X,8HNE     = ,16X,4E16.5)                                   SPE 900
      END                                                                   SPE 910-
```

```
$IBFTC MODE.   LIST,DECK                                                MOD  00
       SUBROUTINE MODE (L)                                              MOD  10
       DIMENSION CO(10),COEF(10)                                        MOD  20
       COMMON /ALL/N,V(100),I(100),ICALC(100),DEL(100,5),IA,IB,VA,      MOD  30
      1 VB,TH,A,B,E,M,ITH,KTR                                           MOD  40
       EQUIVALENCE (COEF(1),IA)                                         MOD  50
       EQUIVALENCE (CO(1),IASAV),(CO(2),IBSAV),(CO(3),VASAV),           MOD  60
      1 (CO(4),VBSAV),(CO(5),THSAV)                                     MOD  70
       REAL I,ICALC,IA,IB,IASAV,IBSAV                                   MOD  80
       DATA CONV/1.0E-3/                                                MOD  90
       ITH=0                                                            MOD 100
10     ITH=ITH+1                                                        MOD 110
       IASAV=IA                                                         MOD 120
       IBSAV=IB                                                         MOD 130
       VASAV=VA                                                         MOD 140
       VBSAV=VB                                                         MOD 150
       THSAV=TH                                                         MOD 160
       KTR=0                                                            MOD 170
20     KTR=KTR+1                                                        MOD 180
       IF (L.EQ.4) GO TO 30                                             MOD 190
       CALL STEADY                                                      MOD 200
       GO TO 40                                                         MOD 210
30     CALL PULSED                                                      MOD 220
40     CALL LESQ                                                        MOD 230
       IF ((ABS(A/VA).LE.CONV).AND.(ABS(B/VB).LE.CONV)) GO TO 50        MOD 240
       IF (KTR.GE.5) GO TO 50                                           MOD 250
       VA=ABS(VA+A)                                                     MOD 260
       VB=VB+B                                                          MOD 270
       GO TO 20                                                         MOD 280
50     KTR=0                                                            MOD 290
60     KTR=KTR+1                                                        MOD 300
       IF (L.EQ.4) GO TO 70                                             MOD 310
       CALL STDY1                                                       MOD 320
       GO TO 80                                                         MOD 330
70     CALL PLSD1                                                       MOD 340
80     CALL LESQ                                                        MOD 350
       IF ((ABS(A/IB).LE.CONV).AND.(ABS(B/TH).LE.CONV)) GO TO 90        MOD 360
       IF (KTR.GE.5.OR.ABS(B).GT.0.5) GO TO 90                          MOD 370
       IB=IB+A                                                          MOD 380
       TH=TH+B                                                          MOD 390
       IF (TH.GT.0.0.AND.TH.LE.1.57079) GO TO 60                        MOD 400
       IB=IB-A                                                          MOD 410
       TH=TH-B                                                          MOD 420
90     X=ABS(IA)                                                        MOD 430
       IX=0                                                             MOD 440
100    IF (X.LT.10.) GO TO 110                                          MOD 450
       IX=IX+1                                                          MOD 460
       X=X/10.                                                          MOD 470
       GO TO 100                                                        MOD 480
110    IF (X.GE.1.0) GO TO 120                                          MOD 490
       IX=IX-1                                                          MOD 500
       X=X*10.                                                          MOD 510
       GO TO 110                                                        MOD 520
120    DIV=10.**IX                                                      MOD 530
       IDIV=0                                                           MOD 540
       INDX=0                                                           MOD 550
       IK=0                                                             MOD 560
130    IK=IK+1                                                          MOD 570
       IF (INDX.GE.50) GO TO 170                                        MOD 580
```

```
      CALL CALC (L,INDX)                                                    MOD 590
      IF (IK.NE.1.AND.E.GE.SE) GO TO 140                                    MOD 600
      SE=E                                                                  MOD 610
      SIA=IA                                                                MOD 620
      GO TO 160                                                             MOD 630
140   IF (IK.NE.2) GO TO 150                                                MOD 640
      DIV=-DIV                                                              MOD 650
      GO TO 160                                                             MOD 660
150   IF (IDIV.GE.2) GO TO 170                                              MOD 670
      IDIV=IDIV+1                                                           MOD 680
      DIV=ABS(DIV/10.)                                                      MOD 690
      IK=1                                                                  MOD 700
160   IA=SIA+DIV                                                            MOD 710
      GO TO 130                                                             MOD 720
170   IA=SIA                                                                MOD 730
      IN=0                                                                  MOD 740
      DO 180 J=1,5                                                          MOD 750
180   IF (ABS((COEF(J)-CO(J))/CO(J)).LE.CONV) IN=IN+1                       MOD 760
      IF (IN.NE.5.AND.ITH.LT.50) GO TO 10                                   MOD 770
      CALL CALC (L,0)                                                       MOD 800
      RETURN                                                                MOD 810
      END                                                                   MOD 820-
```

```
$IBFTC MODE1   LIST,DECK                                                    STD  00
      SUBROUTINE STEADY                                                    STD  10
      REAL I,ICALC,IA,IB                                                   STD  20
      DIMENSION Y(100),TX(100)                                             STD  30
      COMMON /ALL/N,V(100),I(100),ICALC(100),DEL(100,5),IA,IB,VA,          STD  40
     1 VB,ANG,A,B,E,M,KOUNT,KTR                                            STD  50
C                                                                          STD  60
C     DERIVATIVES WITH RESPECT TO VA AND VB                                STD  70
C                                                                          STD  80
10    IF (KTR.GT.1) GO TO 20                                               STD  90
      SA=SIN(ANG)**2                                                       STD 100
      CA=COS(ANG)**2                                                       STD 110
      TA=SA/CA                                                             STD 120
      ZA=IB/SA                                                             STD 130
20    ZB=ZA/VA                                                             STD 140
      DO 40 J=1,N                                                          STD 150
      IF (V(J).LE.VB) GO TO 30                                             STD 160
      X=(V(J)-VB)/VA                                                       STD 170
      EX=EXP(-X)                                                           STD 180
      EXT=EXP(-X*TA)                                                       STD 190
      TXY=ZB*EX*(1.0-EXT)                                                  STD 200
      ICALC(J)=IA+ZA*EX*(1.0-CA*EXT)                                       STD 210
      DEL(J,1)=TXY*X                                                       STD 220
      DEL(J,2)=TXY                                                         STD 230
      GO TO 40                                                             STD 240
30    ICALC(J)=IA+IB                                                       STD 250
      DEL(J,1)=0.0                                                         STD 260
      DEL(J,2)=0.0                                                         STD 270
40    DEL(J,3)=I(J)-ICALC(J)                                               STD 280
      GO TO 100                                                            STD 290
      ENTRY STDY1                                                          STD 300
C                                                                          STD 310
C     DERIVATIVES WITH RESPECT TO IB AND TH                                STD 320
C                                                                          STD 330
      IF (KTR.GT.1) GO TO 70                                               STD 340
      DO 60 J=1,N                                                          STD 350
      IF (V(J).LE.VB) GO TO 50                                             STD 360
      Y(J)=(V(J)-VB)/VA                                                    STD 370
      TX(J)=EXP(-Y(J))                                                     STD 380
      GO TO 60                                                             STD 390
50    DEL(J,1)=1.0                                                         STD 400
      DEL(J,2)=0.0                                                         STD 410
60    CONTINUE                                                             STD 420
70    CA=COS(ANG)                                                          STD 430
      CB=CA**2                                                             STD 440
      SA=SIN(ANG)                                                          STD 450
      SB=SA*SA                                                             STD 460
      SC=SA*SB                                                             STD 470
      CA=0.5*CA*SC                                                         STD 480
      SA=SB/CB                                                             STD 490
      DO 90 J=1,N                                                          STD 500
      IF (V(J).LE.VB) GO TO 80                                             STD 510
      TXY=EXP(-Y(J)*SA)                                                    STD 520
      DEL(J,1)=TX(J)*(1.0-CB*TXY)/SB                                       STD 530
      DEL(J,2)=TX(J)*((CB+Y(J)*SB)*TXY-CB)/CA*IB                           STD 540
80    ICALC(J)=IA+IB*DEL(J,1)                                              STD 550
90    DEL(J,3)=I(J)-ICALC(J)                                               STD 560
100   RETURN                                                               STD 570
      END                                                                  STD 580-
```

```
$IBFTC MODE2   LIST,DECK                                                    PLS  00
       SUBROUTINE PULSED                                                   PLS  10
       REAL I,ICALC,IA,IB                                                  PLS  20
       DIMENSION Y(100),TX(100)                                            PLS  30
       COMMON /ALL/N,V(100),I(100),ICALC(100),DEL(100,5),IA,IB,VA,         PLS  40
      1 VB,ANG,A,B,E,M,KOUNT,KTR                                           PLS  50
C                                                                          PLS  60
C      DERIVATIVES WITH RESPECT TO VA AND VB                               PLS  70
C                                                                          PLS  80
10     IF (KTR.GT.1) GO TO 20                                              PLS  90
       CA=COS(ANG)                                                         PLS 100
       CB=1.0-CA                                                           PLS 110
       CA2=CA**2                                                           PLS 120
       ZB=IB/CB/1.772454                                                   PLS 130
20     ZA=ZB/VA                                                            PLS 140
       DO 40 J=1,N                                                         PLS 150
       IF (V(J).LE.VB) GO TO 30                                            PLS 160
       X2=(V(J)-VB)/VA                                                     PLS 170
       X=SQRT(X2)                                                          PLS 180
       TXY=ZA*(EXP(-X2)-EXP(-X2/CA2))                                      PLS 190
       ICALC(J)=IA+IB*(1.0-(ERF(X)-CA*ERF(X/CA))/CB)                       PLS 200
       DEL(J,1)=X*TXY                                                      PLS 210
       DEL(J,2)=TXY/X                                                      PLS 220
       GO TO 40                                                            PLS 230
30     ICALC(J)=IA+IB                                                      PLS 240
       DEL(J,1)=0.0                                                        PLS 250
       DEL(J,2)=0.0                                                        PLS 260
40     DEL(J,3)=I(J)-ICALC(J)                                              PLS 270
       GO TO 100                                                           PLS 280
       ENTRY PLSD1                                                         PLS 290
C                                                                          PLS 300
C      DERIVATIVES WITH RESPECT TO IB AND TH                               PLS 310
C                                                                          PLS 320
       IF (KTR.GT.1) GO TO 70                                              PLS 330
       DO 60 J=1,N                                                         PLS 340
       IF (V(J).LE.VB) GO TO 50                                            PLS 350
       Y(J)=SQRT((V(J)-VB)/VA)                                             PLS 360
       TX(J)=ERF(Y(J))                                                     PLS 370
       GO TO 60                                                            PLS 380
50     DEL(J,1)=1.0                                                        PLS 390
       DEL(J,2)=0.0                                                        PLS 400
60     CONTINUE                                                            PLS 410
70     SA=SIN(ANG)                                                         PLS 420
       CA=COS(ANG)                                                         PLS 430
       CB=1.0-CA                                                           PLS 440
       CC=IB*SA/CB**2                                                      PLS 450
       CD=1.1283792*CB/CA                                                  PLS 460
       DO 90 J=1,N                                                         PLS 470
       IF (V(J).LE.VB) GO TO 80                                            PLS 480
       X=Y(J)                                                              PLS 490
       XX=ERF(X/CA)                                                        PLS 500
       DEL(J,1)=1.0-(TX(J)-CA*XX)/CB                                       PLS 510
       DEL(J,2)=CC*(CD*EXP(-(X/CA)**2)*X-XX+TX(J))                         PLS 520
80     ICALC(J)=IA+IB*DEL(J,1)                                             PLS 530
90     DEL(J,3)=I(J)-ICALC(J)                                              PLS 540
100    RETURN                                                              PLS 550
       END                                                                 PLS 560-
```

```
$IBFTC CALC1   LIST,DECK                                                CAL  00
      SUBROUTINE CALC (L,INDX)                                          CAL  10
      DIMENSION TX(100)                                                 CAL  20
      REAL I,ICALC,IA,IB,IASAV,IBSAV                                    CAL  30
      COMMON /ALL/N,V(100),I(100),ICALC(100),DEL(100,5),IA,IB,VA,       CAL  40
     1 VB,ANG,A,B,E,M,KOUNT,KTR                                         CAL  50
      E=0.0                                                             CAL  60
      INDX=INDX+1                                                       CAL  70
      IF (INDX.GT.1) GO TO 50                                           CAL  80
      MM=1+L/3                                                          CAL  90
      GO TO (10,30),MM                                                  CAL 100
10    SA=SIN(ANG)**2                                                    CAL 110
      CA=COS(ANG)**2                                                    CAL 120
      TA=SA/CA                                                          CAL 130
      DO 20 J=1,N                                                       CAL 140
      IF (V(J).LE.VB) GO TO 20                                          CAL 150
      X=(V(J)-VB)/VA                                                    CAL 160
      TX(J)=EXP(-X)/SA*(1.0-CA*EXP(-X*TA))                              CAL 170
20    CONTINUE                                                          CAL 180
      GO TO 50                                                          CAL 190
30    CA=COS(ANG)                                                       CAL 200
      CB=1.0-CA                                                         CAL 210
      DO 40 J=1,N                                                       CAL 220
      IF (V(J).LE.VB) GO TO 40                                          CAL 230
      X=SQRT((V(J)-VB)/VA)                                              CAL 240
      TX(J)=1.0-(ERF(X)-CA*ERF(X/CA))/CB                                CAL 250
40    CONTINUE                                                          CAL 260
50    DO 70 J=1,N                                                       CAL 270
      IF (V(J).LE.VB) GO TO 60                                          CAL 280
      ICALC(J)=IA+IB*TX(J)                                              CAL 290
      GO TO 70                                                          CAL 300
60    ICALC(J)=IA+IB                                                    CAL 310
70    E=E+(I(J)-ICALC(J))**2                                            CAL 320
      RETURN                                                            CAL 330
      END                                                               CAL 340-
```

```
$IBFTC LESQ1   LIST,DECK                                                LES  00
      SUBROUTINE LESQ                                                   LES  10
      COMMON /ALL/N,V(100),I(100),ICALC(100),DEL(100,5),IA,IB,VA,       LES  20
     1 VB,ANG,A,B,E,M,KOUNT,KTR                                         LES  30
      DIMENSION SUM(5,6)                                                LES  40
      DO 20 K=1,2                                                       LES  50
      DO 20 J=K,3                                                       LES  60
      SUM(K,J)=0.0                                                      LES  70
      DO 10 L=1,N                                                       LES  80
10    SUM(K,J)=SUM(K,J)+DEL(L,K)*DEL(L,J)                               LES  90
20    SUM(J,K)=SUM(K,J)                                                 LES 100
      A=0.                                                              LES 110
      B=0.                                                              LES 120
      DENOM=SUM(1,1)*SUM(2,2)-SUM(1,2)**2                               LES 130
      IF (DENOM.EQ.0.) GO TO 30                                         LES 140
      A=(SUM(1,3)*SUM(2,2)-SUM(1,2)*SUM(2,3))/DENOM                     LES 150
      B=(SUM(1,1)*SUM(2,3)-SUM(1,3)*SUM(2,1))/DENOM                     LES 160
30    RETURN                                                            LES 170
      END                                                               LES 180-
```

```
$IBFTC SQU     LIST,DECK                                                    SQU  00
      SUBROUTINE SQUARE                                                   SQR  10
      REAL I,ICALC,IA,IB                                                  SQR  20
      COMMON /ALL/N,V(100),I(100),ICALC(100),DEL(100,5),IA,IB,VA,         SQR  30
     1 VB,ANG,A,B,E,M,KOUNT,KTR                                           SQR  40
      DIMENSION COEF(5)                                                   SQR  50
      EQUIVALENCE (IA,COEF(1))                                            SQR  60
      DATA CONV/1.0E-3/                                                   SQR  70
      KOUNT=0                                                             SQR  80
10    KOUNT=KOUNT+1                                                       SQR  90
      SIA=IA                                                              SQR 100
      SIB=IB                                                              SQR 110
      SVA=VA                                                              SQR 120
      SVB=VB                                                              SQR 130
      DO 120 M=1,2                                                        SQR 140
      KTR=0                                                               SQR 150
20    KTR=KTR+1                                                           SQR 160
      VA=ABS(VA)                                                          SQR 170
      VC=2.0*VA+VB                                                        SQR 180
      IF (M.EQ.2) GO TO 70                                                SQR 190
C                                                                         SQR 200
C     DERIVATIVES WITH RESPECT TO VA AND VB.                              SQR 210
C                                                                         SQR 220
      ALPHA=IB/VA/2.0                                                     SQR 230
      KAB=3                                                               SQR 240
      DO 60 J=1,N                                                         SQR 250
      IF (V(J).LE.VB) GO TO 30                                            SQR 260
      IF (V(J).GT.VC) GO TO 40                                            SQR 270
      DEL(J,2)=ALPHA                                                      SQR 280
      DEL(J,1)=DEL(J,2)*(V(J)-VB)/VA                                      SQR 290
      ICALC(J)=IA+DEL(J,2)*(VC-V(J))                                      SQR 300
      GO TO 60                                                            SQR 310
30    ICALC(J)=IA+IB                                                      SQR 320
      GO TO 50                                                            SQR 330
40    ICALC(J)=IA                                                         SQR 340
50    DEL(J,1)=0.0                                                        SQR 350
      DEL(J,2)=0.0                                                        SQR 360
60    DEL(J,3)=I(J)-ICALC(J)                                              SQR 370
      GO TO 110                                                           SQR 380
C                                                                         SQR 390
C     DERIVATIVES WITH RESPECT TO IA AND IB.                              SQR 400
C                                                                         SQR 410
70    KAB=1                                                               SQR 420
      DO 100 J=1,N                                                        SQR 430
      DEL(J,1)=1.0                                                        SQR 440
      IF (V(J).LE.VB) GO TO 80                                            SQR 450
      IF (V(J).GT.VC) GO TO 90                                            SQR 460
      DEL(J,2)=(VC-V(J))/VA/2.0                                           SQR 470
      ICALC(J)=IA+IB*DEL(J,2)                                             SQR 480
      GO TO 100                                                           SQR 490
80    ICALC(J)=IA+IB                                                      SQR 500
      DEL(J,2)=1.0                                                        SQR 510
      GO TO 100                                                           SQR 520
90    ICALC(J)=IA                                                         SQR 530
      DEL(J,2)=0.0                                                        SQR 540
100   DEL(J,3)=I(J)-ICALC(J)                                              SQR 550
110   CALL LESQ                                                           SQR 560
      KAC=KAB+1                                                           SQR 570
      IF ((ABS(A/COEF(KAB)).LE.CONV).AND.(ABS(B/COEF(KAC)).LE.CONV)) GO   SQR 580
```

```
     1TO 120                                                                  SQR 590
      IF (KTR.GE.5) GO TO 120                                                 SQR 600
      COEF(KAB)=COEF(KAB)+A                                                   SQR 610
      COEF(KAC)=COEF(KAC)+B                                                   SQR 620
      GO TO 20                                                                SQR 630
120   CONTINUE                                                                SQR 640
      IF ((ABS((SIA-IA)/SIA).LE.CONV).AND.(ABS((SIB-IB)/SIB).LE.CONV).ANSQR 650
     1D.(ABS((SVA-VA)/SVA).LE.CONV).AND.(ABS((SVB-VB)/SVB).LE.CONV)) GO SQR 660
     2TO 130                                                                  SQR 670
      IF (KOUNT.LT.50) GO TO 10                                               SQR 680
130   RETURN                                                                  SQR 690
      END                                                                     SQR 700-
```

```
$IBFTC FDEL    LIST,DECK                                                      DEL  00
      SUBROUTINE FDELTA                                                      DEL  10
      REAL I,ICALC,IA,IB                                                     DEL  20
      COMMON /ALL/N,V(100),I(100),ICALC(100),DEL(100,5),IA,IB,VA,            DEL  30
     1 VB,ANG,A,B,E,M,KOUNT,KTR                                              DEL  40
      VB=0.0                                                                 DEL  50
      DO 10 J=1,N                                                            DEL  60
      DEL(J,2)=0.0                                                           DEL  70
10    DEL(J,1)=1.0                                                           DEL  80
      KOUNT=0                                                                DEL  90
20    KOUNT=KOUNT+1                                                          DEL 100
      VA=V(KOUNT)                                                            DEL 110
      DEL(KOUNT,2)=1.0                                                       DEL 120
      E=0.0                                                                  DEL 130
      DO 30 J=1,N                                                            DEL 140
      ICALC(J)=IA+IB*DEL(J,2)                                                DEL 150
30    DEL(J,3)=I(J)-ICALC(J)                                                 DEL 160
      CALL LESQ                                                              DEL 170
      IA=IA+A                                                                DEL 180
      IB=IB+B                                                                DEL 190
      DO 40 J=1,N                                                            DEL 200
      ICALC(J)=IA+IB*DEL(J,2)                                                DEL 210
40    E=E+(I(J)-ICALC(J))**2                                                 DEL 220
      IF (KOUNT.EQ.1) GO TO 50                                               DEL 230
      IF (ESAVE.LE.E) GO TO 60                                               DEL 240
50    ESAVE=E                                                                DEL 250
      SIA=IA                                                                 DEL 260
      SIB=IB                                                                 DEL 270
      SVA=VA                                                                 DEL 280
      IF (KOUNT.LT.N) GO TO 20                                               DEL 290
60    IA=SIA                                                                 DEL 300
      IB=SIB                                                                 DEL 310
      VA=SVA                                                                 DEL 320
      DO 70 J=1,N                                                            DEL 330
      ICALC(J)=IA                                                            DEL 340
70    IF (V(J).LT.VA) ICALC(J)=IA+IB                                         DEL 350
      RETURN                                                                 DEL 360
      END                                                                    DEL 370-
```

```
$DATA
AS-3     57   64
   0.      50.     100.     150.     200.     250.     300.     350.
 400.     450.     500.     550.     600.     650.     700.     750.
 800.     850.     900.     950.    1000.    1050.    1100.    1150.
1200.    1250.    1300.    1350.    1400.    1450.    1500.    1550.
1600.    1650.    1700.    1750.    1800.    1850.    1900.    1950.
2000.    2050.    2100.    2150.    2200.    2250.    2300.    2350.
2400.    2450.    2500.    2550.    2660.    2650.    2700.    2750.
2800.    2850.    2900.    2950.    3000.    3050.    3100.    3150.
141.0    134.0    117.8    102.0     92.3     82.5     75.0     69.0
 63.0     56.6     51.75    46.5     44.25    37.5     33.0     30.0
 27.0     25.0     22.5     21.0     19.0     17.0     16.0     14.5
 13.5     12.5     11.0     10.5     10.0      9.0      8.5      7.5
  7.0      6.0      5.5      5.0      4.5      4.0      3.5      3.0
  3.0      2.0      1.0      1.0       .5       .0       .0      -.5
 -1.0     -1.0     -1.5     -1.5     -2.0     -3.0     -3.5     -4.0
 -4.0
 -8.     145.     350.      30.
```

REFERENCES

1. Eubank, Harold P.: Instrumentation for Plasma Diagnostics. Phys. Today, vol. 19, no. 7, July 1966, pp. 91-105.
2. Roth, J. Reece: Modification of Penning Discharge Useful in Plasma Physics Experiments. Rev. Sci. Instr., vol. 37, no. 8, Aug. 1966, pp. 1100-1101.
3. Luce, John S.; et al.: Research in High Temperature Plasma. Rep. AN-1551, Aerojet-General Corp. (AFAPL-TR-67-28), Apr. 1967.
4. Mason, D. W.: An Electrostatic Ion-Energy Analyser. J. Nucl. Energy, Part C, Plasma Phys., vol. 6, 1964, pp. 553-558.
5. Boyd, R. L. F.; and Boylett, F. D. A.: Ion and Electron Energy Distribution in the Hydrogen Discharge. Proc. Roy. Soc., Ser. A, vol. 296, no. 1445, Jan. 17, 1967, pp. 233-42.
6. Leder, Lewis B.; and Simpson, J. Arol: Improved Electrical Differentiation of Retarding Potential Measurements. Rev. Sci. Instr., vol. 29, no. 7, July 1958, pp. 571-574.
7. Orlinov, V.: Concerning the Method of Retardation Curves Obtained With the Aid of an Intermediate Accelerating Grid. Soviet Phys. Solid State, vol. 3, no. 4, Oct. 1961, pp. 880-884.
8. Simpson, J. Arol: Design of Retarding Field Energy Analyzers. Rev. Sci. Instr., vol. 32, no. 12, Dec. 1961, pp. 1283-1293.
9. Simpson, J. Arol; and Marton, L.: Improved Electron Filter Lens. Rev. Sci. Instr., vol. 32, no. 7, July 1961, pp. 802-803.
10. Mendlowitz, H.: Note on Accelerating Components in Particle Spectrometers. Rev. Sci. Instr., vol. 29, no. 8, Aug. 1958, pp. 701-703.
11. Fleischmann, H. H.; Ashby, D. E. T. F.; and Larson, A. V.: Errors in the Use of Mass Analyzers in Plasma Physics. Nucl. Fusion, vol. 5, Dec. 1965, pp. 349-351.
12. Anderson, N.; Eggleton, P. P.; and Keesing, R. G. W.: Magnetic Effects on the Transmission of Electrons Through an Aperture and Their Application to the Retarding-Potential-Difference Technique. Rev. Sci. Instr., vol. 38, no. 7, July 1967, pp. 924-927.
13. Krawec, Roman: An Instrument for Electronic Differentiation of Current-Voltage Characteristics. NASA TN D-2161, 1964.

14. Zubov, Yu. G.; Koltypin, E. A.; Lobikov, E. A.; and Nastyukha, A. I.: Energy Spectrum of the Electrons and Ions Passing Out Through the Ends of a Magnetic Mirror Machine. Soviet Phys.-Tech. Phys., vol. 8, no. 6, Dec. 1963, pp. 513-517.

15. Roth, J. Reece: Nonadiabatic Particle Losses in Axisymmetric and Multipolar Magnetic Fields. NASA TN D-3164, 1965.

16. Roth, J. Reece: Experimental Investigation of Single Interaction Nonadiabatic Losses from Axisymmetric Magnetic Mirrors. Phys. Fluids, vol. 9, no. 12, Dec. 1966, pp. 2538-2540.

17. Sears, Francis W.: An Introduction to Thermodynamics, The Kinetic Theory of Gases, and Statistical Mechanics. Second ed., Addison-Wesley Publ. Co., 1953.

18. Alfvén, Hannes; and Fälthammar, Carl-Gunne: Cosmical Electrodynamics. Second ed., Clarendon Press, 1963, pp. 34-36.

19. Thomas, George B., Jr.: Calculus and Analytic Geometry. Second ed., Addison-Wesley Publ. Co., Cambridge, Mass., 1953.

20. Roth, J. Reece; Freeman, Donald C., Jr.; and Haid, David A.: Superconducting Magnet Facility for Plasma Physics Research. Rev. Sci. Instr., vol. 36, no. 10, Oct. 1965, pp. 1481-1485.

21. Roth, J. Reece: Steady-State, Hot-Ion Particle-Injection Scheme for Mirror Machines. Am. Phys. Soc. Bull., vol. 11, no. 4, June 1966, p. 465.

22. Roth, J. Reece: A New Mechanism for Low Frequency Oscillations in Partially Ionized Gases. Phys. Fluids, vol. 10, no. 12, Dec. 1967, pp. 2712-2714.

23. Roth, J. Reece: Experimental Observation of Nonlinear Oscillations Governed by the Plasma Continuity Equations. Am. Phys. Soc. Bull., vol. 13, no. 2, Feb. 1968, p. 282.

24. Scarborough, James B.: Numerical Mathematical Analysis. Third ed., Johns Hopkins Press, 1955, pp. 451-469.

NASA-Langley, 1968 —— 25 E-4292

NATIONAL AERONAUTICS AND SPACE ADMINISTRATION
WASHINGTON, D. C. 20546

OFFICIAL BUSINESS

FIRST CLASS MAIL

POSTAGE AND FEES PAID
NATIONAL AERONAUTICS AN
SPACE ADMINISTRATION

POSTMASTER: If Undeliverable (Section 15
Postal Manual) Do Not Ret

"The aeronautical and space activities of the United States shall be conducted so as to contribute . . . to the expansion of human knowledge of phenomena in the atmosphere and space. The Administration shall provide for the widest practicable and appropriate dissemination of information concerning its activities and the results thereof."

—NATIONAL AERONAUTICS AND SPACE ACT OF 1958

NASA SCIENTIFIC AND TECHNICAL PUBLICATIONS

TECHNICAL REPORTS: Scientific and technical information considered important, complete, and a lasting contribution to existing knowledge.

TECHNICAL NOTES: Information less broad in scope but nevertheless of importance as a contribution to existing knowledge.

TECHNICAL MEMORANDUMS: Information receiving limited distribution because of preliminary data, security classification, or other reasons.

CONTRACTOR REPORTS: Scientific and technical information generated under a NASA contract or grant and considered an important contribution to existing knowledge.

TECHNICAL TRANSLATIONS: Information published in a foreign language considered to merit NASA distribution in English.

SPECIAL PUBLICATIONS: Information derived from or of value to NASA activities. Publications include conference proceedings, monographs, data compilations, handbooks, sourcebooks, and special bibliographies.

TECHNOLOGY UTILIZATION PUBLICATIONS: Information on technology used by NASA that may be of particular interest in commercial and other non-aerospace applications. Publications include Tech Briefs, Technology Utilization Reports and Notes, and Technology Surveys.

Details on the availability of these publications may be obtained from:

SCIENTIFIC AND TECHNICAL INFORMATION DIVISION

NATIONAL AERONAUTICS AND SPACE ADMINISTRATION

Washington, D.C. 20546